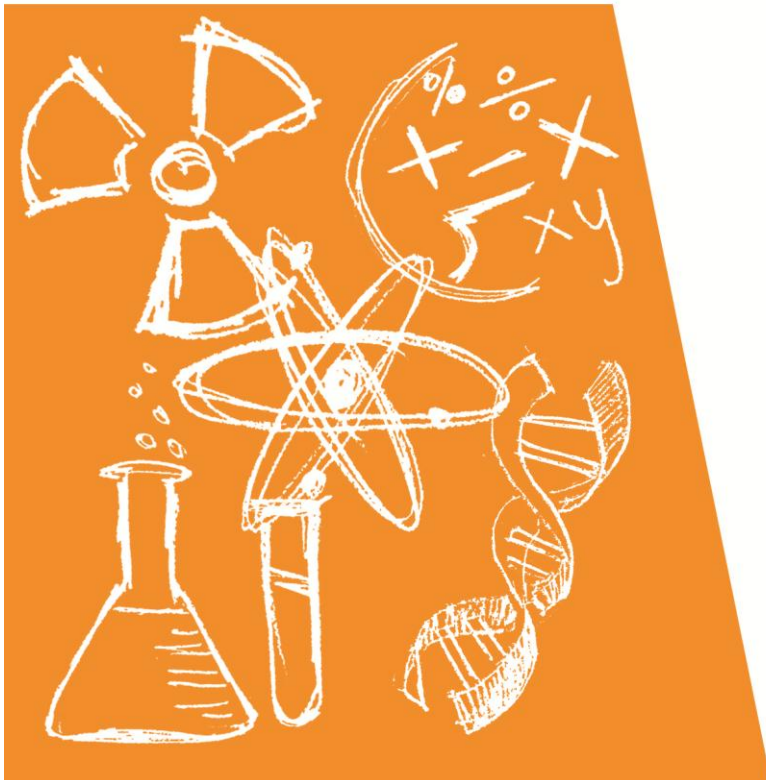


ISSN (E): 2521-2435  
ISSN (P): 2521-2427

The logo for Scientific Inquiry and Review (SIR) features the letters 'SIR' in a stylized font. The 'S' is orange, the 'I' is a vertical bar with horizontal lines, and the 'R' is green. To the right of the letters, the full name 'Scientific Inquiry and Review' is written in a serif font.

**Scientific Inquiry and Review**

**Volume 1 (1) 2017**



**University of Management  
and Technology**

## Scientific Inquiry and Review

Volume 1 Issue 1 2017

### Editorial Team

#### Chief Editor

**Dr. Muhammad Azhar Iqbal**

Professor / Dean School of Science

#### Executive Editor

**Dr. Muhammad Aziz ur Rehman**

Associate Professor

#### Deputy Editors

**Dr. Ayesha Mohy ud Din**

Associate Professor

**Zaheer Hussain Shah**

Assistant Professor

**Muhammad Bilal Riaz**

Assistant Professor

#### Managing Editor

**Muhammad Rafiq Awan**

Director Knowledge & Learning Resources

#### Associate Editors

**Dr. Ehsan Ellahi Khawaja**

Professor / Chairperson Department of  
Physics

**Dr. Sammia Shahid**

Associate Professor

Chairperson Department of Chemistry

**Dr. Muhammad Saeed**

Associate Professor

Chairperson Department of Mathematics

**Dr. Nouman Rasool**

Assistant Professor

Chairperson Department of Life Sciences

#### Assistant Editor

**Fazal Dayan**

Editorial Assistant

### Editorial Board

**Dr. Shaukat Raheem Chowdhury**

Department of Mathematics, UMT

**Dr. M. A. Lodhi**

University of Texas, USA)

**Dr. Cemil Tunc**

Van, Turkey

**Dr. Muhammad Sohail Afzal**

Department of Life Sciences, UMT

**Dr. Azhar Ali Zafar**

GC University, Lahore

**Dr. Narjis Naz**

Lahore College for Women University

**Dr. Laila Zafar**

FC College University, Lahore

**Dr. Amna Mir**

CIIT Lahore

**Dr. Sohail Nadeem**

Department of Chemistry, UMT

**Dr. Naseer Ahmad Asif**

Department of Mathematics, UMT

**Dr. Bertis Little**

University of Louisville, Kentucky, USA

**Dr. Zakia Hammouch Bouhamidi**

Moulay Ismail Meknes Morocco

**Dr. Ebenezer Bonyah**

Kumasi Technical University, Ghana

**Dr. Praveen Agarwal (ANAND)**

International College of Engineering Jaipu

**Dr. Imran Jamil**

Department of Physics, UMT

**Dr. Imran Asjad**

Department of Mathematics, UMT

**Dr. Zaheer-ud-Din Khan**

GC University, Lahore

**Dr. Imran Siddique**

Department of Mathematics, UMT

**Dr. Muhammad Athar Abbasi**

GC University, Lahore

**Mr. Kamran Azhar**

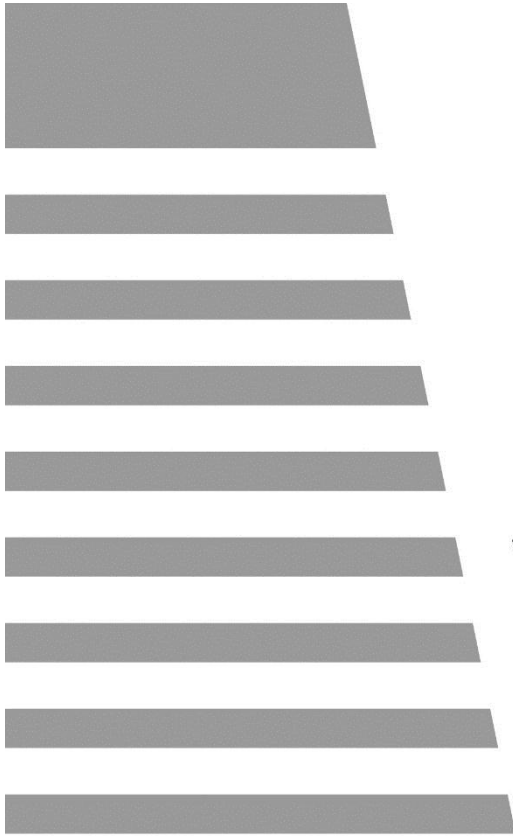
FC College University, Lahore

**Dr. Karl Didcher**

Dalhousie University, Halifax, Canada

**Dr. Erum Akbar Hussain**

Lahore College for Women University



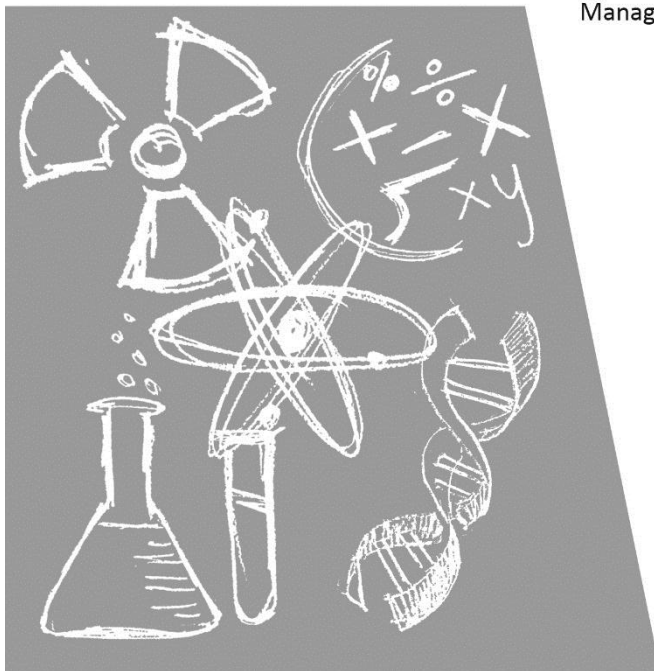
# SIR

Scientific Inquiry and Review

**Volume 1 (1) 2017**

Chief Patron  
Dr. Hasan Sohaib Murad  
Chairman, ILM Trust

Patron  
Dr. Muhammad Aslam  
Rector, UMT  
University of  
Management and Technology



University of Management  
and Technology

# Scientific Inquiry and Review

Volume1, Issue1 2017

**AIMS and SCOPE:** Scientific Inquiry and Review publishes articles in the fields of mathematics, biology, chemistry, physics and other miscellaneous areas of pure and applied sciences.

Manuscripts are categorized into broader areas of pure and applied sciences and may be published as full length articles, short communications/letters, review articles, letter to editor etc. Contributors are encouraged to contact directly to the Chief Editor or editorial team to avoid any conflict about forthcoming publications.

**Electronic Storage or Usage:** Prior permission of publisher is required for electronic storage or usage of any part of journal. No part of journal may be reproduced, stored in any retrieval system or transmitted in any other medium or by any means (electronic, mechanical, photocopying, recording or otherwise) without prior written permission of publisher.

**Disclaimer:** Any article or part of it appearing in the journal is the sole responsibility of author(s) for the content thereof or the damage done to the person/group or property as a matter of product liability, negligence, comment or description or otherwise or ideas contained herein the text. The publication of an article shall not constitute or be deemed to constitute any representation by the Editors, School of Sciences University of Management and Technology that the data presented therein are correct or sufficient to support the conclusions reached or that the experiment design or methodology is adequate.

Published in Islamic Republic of Pakistan  
by the School of Science  
University of Management and Technology  
C- II Johar Town, Lahore Pakistan

Copyright © 2016 University of Management and Technology, Lahore. Published by School of Science, University of Management and Technology, C II Johar Town Lahore. All rights reserved. It is the pre-requisite of publication that the manuscript has not been published or submitted for publication partially or fully anywhere else. After submitting manuscript authors agree that the copyright of their article hereby transferred to the University of Management and Technology, if and when article is accepted for publication.

Cover art copyright © 2016 Office of Communication and Media, UMT

Neither the Chief Editor nor editors assume any liability for statements of fact or opinion made by the authors

All Rights Reserved. Except in certain cases which comply with the fair use guidelines of Pakistan copyright ordinance 1962, no part of this publication may be reproduced, stored in a retrieval system, or transmitted in any form by any means, electronic, mechanical, or otherwise, without the prior permission from the publisher.

All articles appearing in this journal are simultaneously published electronically

®™ The paper used in the publication of journal meets the minimum requirements of ANSI/NISO Z39.48

-1992 (R2009)

**ISSN 2521-2435 (Online)**

**ISSN 2521-2427 (Print)**

## Table of Contents

<b>1</b>	<b>2nd -Order Parallel Splitting Methods for Heat Equation</b> <i>Aziz, M. and Rehman, M. A.</i>	<b>1</b>
<b>2</b>	<b>Generalization of Topsis from Soft Set to Fuzzy Soft Sets in Decision Making Problem</b> <i>Saeed, M., Anam, Z., Kanwal, T. Saba, I. Memoona, F. and Tabassum, M. F.</i>	<b>11</b>
<b>3</b>	<b>Exploration of antibacterial potential of Melia azedarach L.</b> <i>Munir, T.I, Mohyuddin, A., Khan, Z. and Haq, R.</i>	<b>19</b>
<b>4</b>	<b>DFT-Mbj Study of Electronic and Magnetic Properties of Cubic CeCrO<sub>3</sub> Compound: An Ab-Initio Investigation</b> <i>Rashid, M., Iqbal, M.A., and Noor, N. A.</i>	<b>27</b>
<b>5</b>	<b>Opto-Electronic Investigation of Rubidium Based Fluoro-Perovskite for Low Birefringent Lens Materials</b> <i>Iqbal, M. A. and Erum, N.</i>	<b>37</b>
<b>6</b>	<b>Analysis of non-polar chemical profile of Melia azedarach L.</b> <i>Habib, R., Mohyuddin, A. Khan and Mahmood, Z. T.</i>	<b>49</b>



## 2<sup>nd</sup> Order Parallel Splitting Methods for Heat Equation

Aziz, M. <sup>a</sup> and Rehman, M. A. <sup>b</sup>

Department of Mathematics  
University of Management and Technology, Lahore, Pakistan.

azizkb9700@gmail.com<sup>a</sup>, aziz3037@yahoo.com<sup>b</sup>

### Abstract

*In this paper, heat equation in two dimensions with non local boundary condition is solved numerically by 2<sup>nd</sup> order parallel splitting technique. This technique used to approximate spatial derivative and a matrix exponential function is replaced by a rational approximation. Simpson's 1/3 rule is also used to approximate the non local boundary condition. The results of numerical experiments are checked and compared with the exact solution, as well as with the results already existed in the literature and found to be highly accurate.*

**Keywords:** heat equation, 2<sup>nd</sup> order numerical methods, method of lines, parallel algorithm

### Introduction

Several authors have been studied the initial- boundary-value problems (pdes). These equations are mathematical models for real world phenomena which often take the form of equation relating to various quantities and their derivatives. The motion of particle in the straight line, motion of a missile (projectile motion), function of a nuclear reactor, transfer of heat, vibration of a particle and chemical reaction etc. All such problems are governed by elliptic, hyperbolic or parabolic partial differential equations which may or may not be homogenous, in one, two or three dimensions with non local boundary conditions, along with initial conditions existing in the literature. In real life problems, parabolic equations with an integral boundary condition(s) have wide applications, and some time we are required only their numerical solutions. The concentration of a chemical reaction conveniently by employing absorption of light at suitable frequencies. The summation property of electronic and limited availability of light beam, the computational process of used chemical gives rise to quadrature of concentration in spatial region from which the light beam pass through is described by a parabolic equation. We can also use this method for smoothening of data and to calculate time integral of spatial term computation data relating to kinetic rates of chemical reaction. Thus parabolic partial differential equations with nonlocal boundary condition(s) have great impact in diverse fields such as electrochemistry, heat transition, biological and medical sciences and population dynamics. Mostly authors used explicit or Crank-Nikolson finite difference schemes for the numerical solution of these partial differential equations. In 1994

B. J. Noye. et al. have worked out a numerical scheme for the solution of heat equation along with initial condition, boundary conditions and non-local boundary specifications and they used sufficiently smooth data which satisfy the required compatibility conditions in the scheme. They used two different explicit schemes of finite difference which is of second order but for  $S = \frac{1}{6}$  this scheme is of fourth order. They have employed the well-known two finite difference scheme 1<sup>st</sup> is [1], [5] FTCS and 2<sup>nd</sup> is [1], [9] FTCS, and the integral was approximated by Simpson's 1/3 rule to solve the heat equation. He reduced the time consumed 4330.7 sec to 410.3 sec as well as the results were much better than the previous results existing in the literature [2].

The same problem was also discussed by A.B. Gumel. et al.. They replaced the space derivative by central difference approximants of 2<sup>nd</sup> order and approximated the quadrature existing in the recurrence relation by the Trapezoidal rule [3] and the matrix exponential in the recurrence relation by Pade's approximant [4]. They suggested a different scheme to solve the heat equation. [3] used the method of line semi discretization and transformed model PDE into the system of linear, 1<sup>st</sup> order ODE's, and this system of ODE's satisfied a certain recurrence relation. In solution of ODE a matrix exponential term was produced which was approximated with pade approximation, and for unknown  $\omega(t)$ , he used Trapezoidal rule. [3] also presented the result in relative error form and compared with [1], [5] FTCS explicit method . Yunkang Liu worked on heat equation in one dimension with non local boundary conditions. Several authors have discussed PDE's in one dimension as well as in two dimensions with non local boundary conditions [5]. In 1996 Twizell and Taj introduced a new rational approximation to the matrix exponential function, which creates while solving parabolic partial differential equations. In 1997 Taj and Twizell extends their work to fourth-order parallel splitting methods having all properties as in the third order but with much better error of approximation as compared to previous results. These methods do not require any complex arithmetics and are third-order accurate in space and time as well as L-acceptable, tested and found more accurate than the results existing in the literature [9]-[10]. In 2003 Mehdi Dehghan started working on the theory of parallel splitting method and applied this technique for the solution of hyperbolic and parabolic PDEs. Most of his effort appeared from 2003 to 2005 and he used different methods to get a hold for approximate solutions of the heat equation [8]. In 2008 Jurgen Geiser applied fourth order parallel splitting method for the solution of heat equation by using ADI (Alternating Direction Implicit) methods and LOD (Locally One-Dimensional) methods, which are standard splitting methods of lower order, e.g. second order. He extended this second order to fourth order based on locally higher-order LOD methods. In 2007 the heat equation with boundary integral

specification and mixed order parallel splitting method was discussed by M. A. Rehman. For the numerical solution of non classical PDEs, S. Ali Mardan and M. A. Rehman have introduced a hydride method.

We shall use Simpson's 1/3 rule for approximating the integral condition i.e. non-local boundary condition. One way of solving parabolic partial differential equations is by the use of method of lines (MOL), which transform parabolic partial differential equations into a system of ordinary differential equations which can be written in matrix-vector form as

$$\frac{dU(t)}{dt} = BU(t) + \varphi(t) \quad (1)$$

Where  $B$  is a square matrix,  $\varphi(t)$  results from non-homogeneous boundary conditions and  $U(t)$  is the solution vector at time  $t$ .

### Development of the Method

Consider two-dimensional heat equation

$$\frac{\partial u(x, y, t)}{\partial t} = \frac{\partial^2 u(x, y, t)}{\partial x^2} + \frac{\partial^2 u(x, y, t)}{\partial y^2}, \quad 0 < x, y < 1, t > 0 \quad (2)$$

Subject to the given initial condition

$$u(x, y, 0) = g(x, y), \quad 0 \leq x, y \leq 1 \quad (3)$$

and the boundary conditions

$$u(0, y, t) = f_0(y, t), \quad t > 0 \quad (4)$$

$$u(1, y, t) = f_1(y, t), \quad t > 0 \quad (5)$$

$$u(x, 1, t) = g_1(x, t), \quad t > 0 \quad (6)$$

$$u(x, 0, t) = g_0(x)\omega(t), \quad t > 0 \quad (7)$$

With nonlocal boundary condition

$$\iint_{00}^{11} u(x, y, t) dx dy = \mu(t) \quad 0 \leq x, y \leq 1 \quad (8)$$

Where

$$f_0(y, t), f_1(y, t), g_0(x, t), g_1(x, t) \text{ and}$$

$\mu(t)$  are functions which are continuous and known, where as  $u$  and  $\omega$  are the unknown functions to be determined.

### Discretization

The intervals  $0 \leq x \leq 1$  and  $0 \leq y \leq 1$  are divided into  $N + 1$  subintervals of equal length  $h$  and  $h = \frac{1}{N+1}$  and  $t$  is the time variable and length of each time step is equal and is  $l$ , and occupying space  $R = [0 < x < 1] \times [0 < y < 1] \times [t > 0]$  gives a cuboidal mesh of cuboids of equal volume  $h^2 \times l$  and the co-ordinates of

vertices of each cuboids are  $(x_m, y_m, t_n) = (mh, mh, nl)$  where  $m = 0, 1, 2, 3, \dots, N + 1$  and  $n = 0, 1, 2, 3, \dots$ . The boundary  $\partial R$  of whole space is consisting of lines  $x = 0, x = 1, y = 0, y = 1$  and  $t = 0$ .

### Derivation

The space derivative  $\frac{\partial^2 u(x,y,t)}{\partial x^2}$  and  $\frac{\partial^2 u(x,y,t)}{\partial y^2}$ , are approximated as under

$$\frac{\partial^2 u(x,y,t)}{\partial x^2} = \frac{1}{h^2} \{u(x-h, y, t) - 2u(x, t) + u(x+h, y, t)\} + O(h^3) \quad (9)$$

and

$$\frac{\partial^2 u(x,y,t)}{\partial y^2} = \frac{1}{h^2} \{u(x, y-h, t) - 2u(x, t) + u(x, y+h, t)\} + O(h^3) \quad (10)$$

Applying these approximations to the each mesh points of the grid, at time level  $t = t_n$ , we get a system of  $N^2$  first-order ordinary differential equations. This may be written in matrix form as

$$\frac{dU(t)}{dt} = BU(t) + \varphi(t), \quad t > 0$$

With initial distribution

$$U(0) = g(x, y)$$

The matrix B is the sum of two square matrices  $B_1$  and  $B_2$  of order  $N^2$ .

$$B_1 = \frac{1}{h^2} \begin{bmatrix} h^2 A & & & & O \\ & h^2 A & & & \\ & \ddots & \ddots & \ddots & \\ & & & h^2 A & \\ O & & & & h^2 A \end{bmatrix}$$

where A is given by

$$A = \frac{1}{h^2} \begin{bmatrix} -2 & 1 & & & O \\ 1 & -2 & 1 & & \\ & \ddots & \ddots & \ddots & \\ & & & 1 & -2 & 1 \\ O & & & & 1 & -2 \end{bmatrix}$$

and

$$B_2 = \frac{1}{h^2} \begin{bmatrix} -2I & I & & O \\ I & -2I & I & \\ & \ddots & \ddots & \ddots \\ & & I & -2I & I \\ O & & & I & -2I \end{bmatrix}$$

Where both  $B_1$  and  $B_2$  are of order  $N^2 \times N^2$  and  $I$  is the identity matrix of order  $N$ . The vector  $\varphi(t)$ , sum of two vectors  $\varphi_1(t)$  and  $\varphi_2(t)$  of order  $N^2 \times 1$  arises from the use of the boundary conditions in above two approximation.

Then solution  $U(t)$  satisfies the recurrence relation

$$U(t+l) = \exp(lB)U(t) + \int_t^{t+l} \exp((t+l-s)B)\varphi(s) ds; \quad t = 0, l, 2l, \dots$$

Where  $l$  is constant time step in the descretization. To approximate the matrix exponential function in a new rational approximate, for a real scalar  $\theta$ , given by

$$E_2(\theta) = \frac{1 + (1-a)\theta + (a - \frac{1}{2})\theta^2}{1 - a\theta + (a - \frac{1}{2})\theta^2}$$

The unknown  $U^n$  will be ordered in the form

In which  $(t) = [U_{1,1}(t), U_{2,1}(t), U_{3,1}(t), \dots, U_{N,1}(t), \dots, U_{1,N}(t), U_{2,N}(t), \dots, U_{N,N}(t)]^T$ ,

$$g = [g_{1,1}, g_{2,1}, g_{3,1}, \dots, g_{N,1}, \dots, g_{1,N}, g_{2,N}, \dots, g_{N,N}]^T$$

and the solution of system satisfy the recurrence relation (2). Where

$$\int_t^{t+l} \exp((t+l-s)B)\varphi(s) ds = W_1\varphi(s_1) + W_2\varphi(s_2)$$

Where  $s_1 \neq s_2$  and weights  $W_i (i = 1, 2, \dots)$  are matrices. It can easily be shown that when

$$\varphi(s) = [1, 1, 1, \dots, 1]^T, \text{ then}$$

$$W_1 + W_2 = M_1$$

where

$$M_1 = \{B^{-1}(\exp(lB) - I)\}$$

and when

$$\varphi(s) = [s, s, s, \dots, s]^T, \text{ then}$$

$$S_1 W_1 + S_2 W_2 = M_2$$

where  $M_2 = B^{-1} \{ t \exp(lB) - (t+l)I + B^{-1}(\exp(lB) - I) \}$

$$\text{Using } \theta = lB \text{ in } E_2(\theta) = \frac{1+(1-\alpha)\theta + \exp(lB) = PQ \text{ we have}}{1-\alpha\theta + (\alpha - \frac{1}{2})\theta^2}$$

$$P(lB) = (I - \alpha lB + ((\alpha - \frac{1}{2})l^2 B^2)^{-1}$$

and

$$Q(lB) = I + (1 - \alpha)lB$$

Taking  $s_1 = t, s_2 = t + l$   
and then solving and replacing by  $\exp(lB)$  gives

$$U(t+l) = \exp(lB)U(t) + \frac{l}{2} [G(lB)\varphi(t) + K(lB)\varphi(t+l)]; t = 0, l, 2l, \dots$$

$$\text{In which, } G(lB) = \left[ I - \alpha lB + (\alpha - \frac{1}{2})(lB)^2 \right]^{-1}$$

And

$$K(lB) = \left[ I - \alpha lB + (\alpha - \frac{1}{2})(lB)^2 \right]^{-1} \left[ I - 2(\alpha - \frac{1}{2})lB \right]$$

### Parallel Algorithm

In parallel Algorithm  $\exp(lB)$ ,  $G(lB)$  and  $(lB)$  are decomposed in their partial fraction form given below

$$\exp(lB) = \sum_{i=1}^2 q_i (I - \lambda_i lB)^{-1}$$

Where

$$q_1 = \frac{1 - \alpha + \lambda_1}{\lambda_1 - \lambda_2}, q_2 = \frac{1 - \alpha + \lambda_2}{\lambda_2 - \lambda_1}$$

and

$$G(lB) = \sum_{i=1}^2 q_{i+2} (I - \lambda_i lB)^{-1}$$

Where

$$q_3 = \frac{\lambda_1}{\lambda_1 - \lambda_2}, q_4 = \frac{\lambda_2}{\lambda_2 - \lambda_1}$$

$$K(lB) = \sum_{i=1}^2 q_{i+4} (I - \lambda_i lB)^{-1}$$

where

$$q_5 = \frac{1-2\alpha + \lambda_1}{\lambda_1 - \lambda_2}, q_6 = \frac{1-2\alpha + \lambda_2}{\lambda_2 - \lambda_1}$$

Where  $\lambda_1$  and  $\lambda_2$  are given below

$$\lambda_1 = \frac{2\alpha - 1}{\alpha + \sqrt{\alpha^2 - 4\alpha + 2}}$$

and

$$\lambda_2 = \frac{2\alpha - 1}{\alpha - \sqrt{\alpha^2 - 4\alpha + 2}}$$

Hence equation

$$U(t+l) = \exp(lB)U(t) + \frac{l}{2}[G(lB)\varphi(t) + K(lB)\varphi(t+l)]; t = 0, l, 2l, \dots$$

become

$$U(t+l) = \sum_{i=1}^2 A_i^{-1}(q_i U(t) + \frac{l}{2}(q_{i+2}\varphi(t) + q_{i+4}\varphi(t+l)))$$

Where

$$A_i = (I - \lambda_i l B)^{-1}, i = 1, 2$$

Hence

$$U(t+l) = \sum_{i=1}^2 y_i(t)$$

Where  $y_i$  are the solutions of the system.

$$A_i y_i = q_i U(t) + \frac{l}{2}\{q_{i+2}\varphi(t) + q_{i+4}\varphi(t+l)\}$$

### **Numerical Experiment**

$$u(x, y, t) = e^{x+y}$$

$$u(0, y, t) = e^{y+2t}$$

$$u(1, y, t) = e^{1+y+2t}$$

$$u(x, 1, t) = e^{1+x+2t}$$

$$u(x, 0, t) = g_0(x)\omega(t)$$

$$g_0(x) = e^x$$

$$\mu(t) = (e-1)^2 e^{2t}$$

$$\omega(t) = e^{2t}$$

The analytical solution of the problem is

$$u(x, y, t) = e^{x+y+2t}$$

Table 1.

Relative errors for  $n = 49$  and  $l = \frac{1}{15000}$  when  $\omega(t)$  is given

Node points $x = y$	Theoretical solution	2nd order finite difference [3]	New Scheme
0:1	9.0250	$2:5562 \times 10^{-7}$	$1.171 \times 10^{-6}$
0:2	11.0232	$2:8302 \times 10^{-6}$	$2.881 \times 10^{-6}$
0:3	13.4637	$4:1114 \times 10^{-6}$	$4.151 \times 10^{-6}$
0:4	16.4446	$4:6798 \times 10^{-6}$	$4.714 \times 10^{-6}$
0:5	20.0855	$4:5541 \times 10^{-6}$	$4.586 \times 10^{-6}$
0:6	24.5325	$3:8804 \times 10^{-6}$	$3.913 \times 10^{-6}$
0:7	29.9641	$2:8540 \times 10^{-6}$	$2.890 \times 10^{-6}$
0:8	36.5982	$1:6804 \times 10^{-6}$	$1.722 \times 10^{-6}$
0:9	44.7012	$1:0154 \times 10^{-6}$	$6.340 \times 10^{-7}$

### The Treatment of Non Local Boundary Condition

By using Simpson's 1/3 Rule.

$$\int_0^1 \int_0^1 u(x, y, t) dx dy \approx \frac{h^2}{9} \sum_{i=0}^M \sum_{j=0}^M b_i b_j U_{i,j}$$

Where

$$M = N + 1$$

$$b_0 = b_M = 1$$

$$c_i = 4 \text{ for odd } i \text{ and } c_i = 2 \text{ for even } i$$

Above equation may be written as

$$\int_0^1 \int_0^1 u(x, y, t) dx dy \approx \frac{h^2}{9} \sum_{i=0}^M c_i U_{i,0} + R(t)$$

Where

$$R(t) = \frac{h^2}{9} \sum_{i=0}^M \sum_{j=1}^M c_i c_j U_{i,j}$$

Integrating the boundary condition with respect to  $x$  it gives

$$\int_0^1 u(x, 0, t) = \omega(t) \int_0^1 g_0(x) dx$$

Once again use Simpsons' Rule we get

$$\frac{h}{3} \sum_{i=0}^M c_i U_{i,0} \approx \omega(t) \int_0^1 g_0(x) dx$$

$$\omega(t) = \frac{\mu(t) - R(t)}{\frac{h}{3} \left( \int_0^1 \int_0^1 g_0(x) dx \right)}$$

Table2.

Relative errors for  $n = 49$  and  $l = \frac{1}{15000}$  When  $\omega(t)$  is unknown

Node points $x = y$	Theoretical solution	2nd order finite difference [3]	New Scheme with Simpson's rule
0:1	9.0250	$3:3994 \times 10^{-4}$	$6.049 \times 10^{-6}$
0:2	11.0232	$3:0427 \times 10^{-6}$	$3.207 \times 10^{-6}$
0:3	13.4637	$2:6002 \times 10^{-4}$	$5.420 \times 10^{-7}$
0:4	16.4446	$1:8408 \times 10^{-4}$	$1.422 \times 10^{-6}$
0:5	20.0855	$1:1595 \times 10^{-4}$	$2.512 \times 10^{-6}$
0:6	24.5325	$6:3782 \times 10^{-5}$	$2.764 \times 10^{-6}$
0:7	29.9641	$2:9338 \times 10^{-5}$	$2.349 \times 10^{-6}$
0:8	36.5982	$5:1982 \times 10^{-6}$	$1.526 \times 10^{-6}$
0:9	44.7012	$3:3960 \times 10^{-6}$	$5.940 \times 10^{-7}$

### Conclusion

Using given algorithm the problems are solved for  $n = 49$  and  $l = \frac{1}{15000}$ . We have developed 2<sup>nd</sup> order parallel splitting method for heat equation in two dimensions and non local boundary condition was approximated by Simpson's 1/3 rule and exponential term in recurring relation by new rational approximate. First we solved the problem when the value of  $\omega(t)$  was given and then for unknown  $\omega(t)$ . The method is  $L_0$  stable and used for two dimensional heat equation with non local boundary conditions. The results for relative error obtained by using above numerical method compared with the results [3], which are better. It is also observed that there is no oscillation over the entire interval and the method behaved smoothly.

### References

- [1] Degan G. Parabolic equation and thermodynamics. *Quart Appl Math.* 1992;50:523–533.
- [2] Noye BJ, Deghan M, Van J, Hoek D. Explicit finite difference method for two dimension diffusion with non local boundary condition. *Int J Eng Sci.* 1994;32(11):1829–184.
- [3] Gumel AB, Ang WT, Twizell EH. Efficient parallel algorithm for two dimensional diffusion equation subject to specification mass. *Int J Comput Math.* 1997;64(1–2):153–163.
- [4] Twizell EH. *Computational methods for partial differential equations.* Chichester, West Sussex: Ellis Horwood; 1984.
- [5] Liu Y. Numerical solution of the heat equation with nonlocal boundary conditions. *J Comput Appl Math.* 1999;110(1):115–127.
- [6] Borovykh N. Stability in the numerical solution of the heat equation with nonlocal boundary conditions. *Appl Numer Math.* 2002;42(1–3):17–27.
- [7] Geiser J. Fourth–order splitting methods for time dependent differential equations. *Numer Math Theor Appl.* 2008;1(3):321–339.
- [8] Day WA. Extension of a property of the heat equation to linear thermo elasticity and other theories. *Quart Appl Math.* 1982;40(3):319–330.
- [9] Deghan M. Efficient techniques for the second-order parabolic equation subject to nonlocal specifications. *Appl Numer Math.* 2005;52(1):39–62.
- [10] Taj MS, Twizell EH. A family of third-order parallel splitting methods for parabolic partial differential equations. *Int J Comput Math.* 1998;67(3–4):411–433.
- [11] Taj MS, Twizell EH. A family of fourth-order parallel splitting methods for parabolic partial differential equations. *Int J Comput Math.* 1998;67(3–4):357–373.
- [12] Wang S, Lin Y. A numerical method for the diffusion equation with nonlocal boundary specifications. *Inter J Eng Sci.* 1990;28:543–546.

## Generalization of TOPSIS from Soft Set to Fuzzy Soft Sets in Decision Making Problem

Saeed, M., Anam, Z., Kanwal, T., Saba, I., Memoona, F. and Tabassum, M. F.\*

Department of Mathematics, School of Sciences, University of Management and  
Technology, Lahore, Pakistan

\* farhanuet12@gmail.com

### Abstract

*As of late, the issue of basic decision making has discovered imperative centrality. It has procured central significance particularly for the issues identified with incorrect environment. The technique for order of preference by similarities to ideal solution (TOPSIS) is the multi criteria choice examining technique utilized for the choice. We apply the generalized result of TOPSIS on soft set to TOPSIS on fuzzy-soft-set.*

**Keywords:** TOPSIS, Soft-sets (SS), fuzzy-soft-sets (FSS), weighted-normalized-decision-matrix (WNDM) and fuzzy-sets (FS).

### Introduction

In real life, we face many problems of decision making in different domains of sciences such as engineering, medical science and economics. To address uncertain situation and treat ambiguous data, Zadeh [1] presented the idea of fuzzy sets in 1965. Introduction of fuzzy set theory revolutionized the entire mathematical sciences. Many researchers contributed in the development of fuzzy sets and its applications in various fields of life.

In 1980 Thomas Saaty [2] introduced Analytical Hierarchy process. These are most useful techniques for dealing difficult decision making and help the decision makers to make accurate decisions. This theory consists of many applications such as, medicine, computer science, control engineering and artificial intelligence etc.

To ease this situation of decision making a methodology was developed by Hwang and Yoon [3] in 1981, named as TOPSIS. But TOPSIS on soft set is useful for discrete situations. In 1999 Molodtsov proposed the theory of soft-sets as a generalization of fuzzy set, which can efficiently handle a number of parameters simultaneously.

The idea of fuzzy-soft-set was first presented by Maji et al. in 2001. In 2002, firstly the technique of fuzzy-soft-set was used in decision making. In 2013, Maji et al. presented the idea of the neutrosophic-soft-set. For decision making many techniques are used such as soft expert set, AHP, interval valued fuzzy soft

matrix, TOPSIS etc. These techniques are proved to be very helpful in decision making. M. Saeed, Sana. A. and N. Rubi [4] compared the two different technique , fuzzy-soft-expert-set and AHP. The computational cost of Fuzzy-Soft-Expert-Set system is minimum than AHP procedure for the same outcome. They conclude that AHP and fuzzy-soft-expert-set gives the same result.

Zulqarnain. M and M. Saeed [5] have applied fuzzy-soft-set in decision making. The idea of fuzzy-soft-set has been presented earlier [6]. But decision making on fuzzy-soft-set by applying TOPSIS is presented for the first time in this paper. In this paper, we generalized the concept of TOPSIS from soft-set to fuzzy-soft-sets in decision making. In this paper the author present some basic concepts associated to soft-set and fuzzy-soft-set and procedure of TOPSIS. Also develop the methodology of decision making via TOPSIS on fuzzy-soft-set and conclude the results.

## 2. Preliminaries

In this subcategory, we present the fundamental concepts and outcomes of soft-set-theory, which would be beneficial for additional dialogues. Maximum descriptions and outcomes obtainable in this subdivision may be established in [7-9].

### Definition1

“Let  $S$  be a set of parameters and  $W$  be an initial universe set. Let  $W$  be the power set denoted by  $P(U)$  the and  $A \subset S$ . A pair  $(G, A)$  is called a soft set over  $W$ , given by

$$G: A \rightarrow P(U)''$$

Where  $G$  is a mapping [10]

### Fuzzy-Soft-Set in Decision-Making

In this section, we will discuss some elementary description of fuzzy soft set (FSS) and some outcomes, which we use in further debate. Most of them are originating in [11,12].

The parameter space  $S$  may be written as

$$S \supseteq \{ B_1 \cup B_2, \dots, \cup B_i \}.$$

Let each parameter set  $Y_j$  characterize the  $j^{\text{th}}$  class of parameters and the elements of  $B_j$  represents a particular property set. Here we suppose that these property sets may be observed as fuzzy-sets (FS).

### Definition2

“Let  $P(V)$  represents the set of complete fuzzy-set of  $V$ . Let  $X_i \subset E$ . A pair is  $(H_i, X_i)$  is called a fuzzy-soft-set over  $V$ . We may now describe a FSS  $(G_j, B_j)$  which illustrates a set of objects having the parameter set [13], where  $H_i$  is a mapping given by  $H_i : X_i \rightarrow P(V)$ . [14]

### TOPSIS

The basic steps of TOPSIS are described in [15]

**Stage1.** First determine the normalized-decision-matrix.

The normalized value is denoted by  $x_{ij}$  is calculated as follows:

$$x_{ij} = y_{ij} \sqrt{\sum_{i=1}^n y_{ij}^2} \quad i=1, 2, \dots, n \text{ and } j = 1, 2, \dots, m.$$

**Stage 2.** Evaluate the weighted normalized decision-matrix. The weighted normalized value  $U_{ij}$  is calculated as follows:

$$U_{ij} = X_{ij} \times W_i, \\ i=1, 2, \dots, n \text{ and } j = 1, 2, \dots, m. \quad [16]$$

where  $W_i$  is the weight of the  $i^{\text{th}}$  alternative and  $\sum_{i=1}^n W_i = 1$ .

**Stage3.** Calculate the best ideal solution ( $B^*$ ) and worst ideal ( $B^-$ ) solutions [17, 18].

$$B^* = \{(\max_i u_{ij} | i \in D_a), (\min_i u_{ij} | i \in D_c)\} = \{u_i^* | i=1, 2, \dots, n\} \\ B^- = \{(\min_i u_{ij} | i \in D_b), (\max_i u_{ij} | i \in D_c)\} = \{u_i^- | i=1, 2, \dots, n\}$$

**Stage4.** By using the n-dimensional Euclidean space compute the distance. The parting procedures of each substitute from the best-ideal-solution and the worst-ideal-solution, respectively, as given below: [19, 20]

$$D_i^* = \sqrt{\sum_{i=1}^n (u_{ij} - u_i^*)^2}, i=1, 2, \dots, n \\ D_i^- = \sqrt{\sum_{i=1}^n (u_{ij} - u_i^-)^2}, i=1, 2, \dots, n$$

**Stage5.** Compute the relative closeness to the best-ideal-solution. The relative closeness of the alternative with respect  $X_i$  to  $B^*$  is defined as follows [21]:

$$RC_i^* = \frac{D_i^-}{D_i^* + D_i^-}, i=1, 2, \dots, n$$

**Stage 6.** Rank the preference order.

#### A Decision Making Method on Fuzzy Soft Set

In this section, we deliberate the decision-making method by using TOPSIS on soft-set-theory. The detailed method, of each step, is shown below.

**Step1.** Defining the problem. Let us assume that

$$DM = \{D_p, p \in I_n\} \text{ are the sets of decision makers,} \\ v = \{v_i, i \in I_m\} \text{ denote the set of alternatives}$$

and  $x = \{x_{j,j} \in I_n\}$  is set of all parameters. Then FSS over  $v$  is a function defined by

$$H_i : X_i \rightarrow P(V)$$

where  $H_i$  a mapping is given by [22]

**Step2.** Construct decision matrix D for each decision makers.

Where  $D = V_{i,j \in I_n} d_{ij}$ ,  $d_{ij} = f_{x_i}(x_j)$  is the criterion values of  $i^{th}$  alternatives received from the criterion,  $X_i$  is the parameter sets of decision makers  $D_p$  and  $f_{x_i}$  is the soft set which was constructed by  $D_p$ .

$$D = \begin{matrix} & x_1 & x_2 & \cdots & x_n \\ \begin{matrix} v_1 \\ v_2 \\ \vdots \\ v_m \end{matrix} & \begin{bmatrix} d_{11} & d_{12} & \cdots & d_{1n} \\ d_{21} & d_{22} & \cdots & d_{2n} \\ \vdots & \vdots & \cdots & \vdots \\ d_{m1} & d_{m2} & \cdots & d_{mn} \end{bmatrix} & = & [d_{ij}]_{m \times n} \end{matrix}$$

**Step3:** Obtaining the WNDM of V. The WNDM is calculated as:

$$V = \begin{matrix} & \begin{bmatrix} v_{11} & v_{12} & \cdots & v_{1n} \\ v_{21} & v_{22} & \cdots & v_{2n} \\ \vdots & \vdots & \cdots & \vdots \\ v_{m1} & v_{m2} & \cdots & v_{mn} \end{bmatrix} \\ = & [v_{ij}]_{m \times n} \end{matrix}$$

where  $v_{kt} = \sum_{i=1}^n f_{x_i}(x_k)(u_t)$ ,  $\forall i, k, t \in I_n$

**Step4.**

$$k(u_j) = \sum_{i=1}^n v_{ji}$$

where,  $k(u_j)$  is decision values of  $u_j$ . Thus the decision matrix of each alternative values for the deciders is expressed as

$$R = \{k(u_1), \dots \dots \dots k(u_n)\}$$

**Step5.** Ranking the preference order.

### An Application

**Step1. Defining the problem**

Suppose that a car dealer has a set of various types of cars (universal set-alternatives)

$$v = \{v_1, v_2, v_3\}$$

which may be categorized by a set of all parameters

$$Y = \{y_1, y_2, y_3\} \text{ For } j = 1, 2, 3.$$

The parameters  $Y_j$  stand for "luxuries", "automatic" and "manual" respectively.

Assume that three decision-makers come to the car dealer to buy a car.

Firstly, each decision-maker has their own choice about car and they consider their own set of parameters.

Then they can construct their fuzzy-soft-sets. Next, by using the fuzzy-soft-set and TOPSIS-decision making method we select a car on the basis of parameters of decision makers.

**Step2.** Construct decision matrix D for each decision-makers. We can construct fuzzy soft sets of decision-makers,  $D_i$  in a tabular form respectively as Fuzzy soft sets of decision-maker,  $D_1$  is

$$\begin{array}{c} y_1 \quad y_2 \quad y_3 \\ v_1 \begin{bmatrix} 0.3 & 0.5 & 0.2 \end{bmatrix} \\ v_2 \begin{bmatrix} 0.2 & 1 & 0 \end{bmatrix} \\ v_3 \begin{bmatrix} 0.4 & 0 & 0.3 \end{bmatrix} \end{array}$$

Fuzzy soft sets of decision-maker,  $D_2$  is

$$\begin{array}{c} y_1 \quad y_2 \quad y_3 \\ v_1 \begin{bmatrix} 0.2 & 0.5 & 0.4 \end{bmatrix} \\ v_2 \begin{bmatrix} 0.3 & 0 & 2 \end{bmatrix} \\ v_3 \begin{bmatrix} 0.1 & 0.5 & 0.4 \end{bmatrix} \end{array}$$

Fuzzy soft sets of decision-maker,  $D_3$  is

$$\begin{array}{c} y_1 \quad y_2 \quad y_3 \\ v_1 \begin{bmatrix} 0.4 & 0 & 0.3 \end{bmatrix} \\ v_2 \begin{bmatrix} 0.5 & 0 & 0.1 \end{bmatrix} \\ v_3 \begin{bmatrix} 0.4 & 0.2 & 0.1 \end{bmatrix} \end{array}$$

**Step3.** Creating the weighted-normalized-decision-matrix V.

Now compute the weights corresponding to each parameter.

$$\begin{aligned} v_{11} &= \sum_{i=1}^3 f_{y_i(y_1)}(v_1) = f_{y_1(y_1)}(v_1) + f_{y_2(y_1)}(v_1) + f_{y_3(y_1)}(v_1) \\ &= 0.3 + 0.2 + 0.4 = 0.9 \end{aligned}$$

$$\begin{aligned} v_{12} &= \sum_{i=1}^3 f_{y_i(y_2)}(v_2) = f_{y_1(y_2)}(v_2) + f_{y_2(y_2)}(v_2) + f_{y_3(y_2)}(v_2) \\ &= 0.2 + 0.3 + 0.5 = 1 \end{aligned}$$

$$v_{13} = \sum_{i=1}^3 f_{y_i(y_3)}(v_3) = f_{y_1(y_3)}(v_3) + f_{y_2(y_3)}(v_3) + f_{y_3(y_3)}(v_3)$$

$$\begin{aligned}
 &= 0.4 + 0.1 + 0.4 = 0.9 \\
 v_{21} &= \sum_{i=1}^3 f_{y_i(y_2)}(v_1) = f_{y_1(y_2)}(v_1) + f_{y_2(y_2)}(v_1) + f_{y_3(y_2)}(v_1) \\
 &= 0.5 + 0.5 + 0 = 01 \\
 v_{22} &= \sum_{i=1}^3 f_{y_i(y_2)}(v_2) = f_{y_1(y_2)}(v_2) + f_{y_2(y_2)}(v_2) + f_{y_3(y_2)}(v_2) \\
 &= 0.0 + 0.0 + 01 = 01 \\
 v_{23} &= \sum_{i=1}^3 f_{y_i(y_2)}(v_3) = f_{y_1(y_2)}(v_3) + f_{y_2(y_2)}(v_3) + f_{y_3(y_2)}(v_3) \\
 &= 0.0 + 0.5 + 0.2 = 0.7 \\
 v_{31} &= \sum_{i=1}^3 f_{y_i(y_3)}(v_1) = f_{y_1(y_3)}(v_1) + f_{y_2(y_3)}(v_1) + f_{y_3(y_3)}(v_1) \\
 &= 0.2 + 0.4 + 0.3 = 0.9 \\
 v_{32} &= \sum_{i=1}^3 f_{y_i(y_3)}(v_2) = f_{y_1(y_3)}(v_2) + f_{y_2(y_3)}(v_2) + f_{y_3(y_3)}(v_2) \\
 &= 0.0 + 0.2 + 0.1 = 0.3 \\
 v_{33} &= \sum_{i=1}^3 f_{y_i(y_3)}(v_3) = f_{y_1(y_3)}(v_3) + f_{y_2(y_3)}(v_3) + f_{y_3(y_3)}(v_3) \\
 &= 0.3 + 0.4 + 0.1 = 0.8
 \end{aligned}$$

Then the weight matrix is obtained as

$$V = \begin{bmatrix} 0.9 & 1 & 0.9 \\ 0.1 & 1 & 0.7 \\ 0.9 & 0.3 & 0.8 \end{bmatrix}$$

**Step4:** Creating the decision matrix (vector), R.

Now, calculate the individual elements of the R matrix.

$$k(v_1) = \sum_{i=1}^3 v_{1i} = v_{11} + v_{12} + v_{13} = 0.9 + 0.1 + 0.9 = 2.8$$

$$k(v_2) = \sum_{i=1}^3 v_{1i} = v_{21} + v_{22} + v_{23} = 0.1 + 0.1 + 0.3 = 2.3$$

$$k(v_3) = \sum_{i=1}^3 v_{1i} = v_{31} + v_{32} + v_{33} = 0.9 + 0.7 + 0.8 = 2.4$$

$$R = [2.8, 2.3, 2.4]$$

**Step 5.** Ranking the preference order.

Ranking of the alternatives would be created in the descending order of the values  $k(v_j)$  calculated in the fifth step. So when the fifth step in the calculation of the evaluation of the candidate cars (alternatives) from small to large  $k(v_2) < k(v_3) < k(v_1)$ , the order form is realized in the form of ranking  $v_2 < v_3 < v_1$ . In other words, the most suitable car appears to be  $v_1$ .

### 3. Conclusion

We proposed a new method for selection in this paper. After verifying the accumulations on different situations it can be observed that the new method is quite simple to use and significant for accumulation. Also, it has less no of calculations than the original TOPSIS. In this method we deal with the indeterminate and fuzzy or ambiguous values. We get same result through soft set on TOPSIS and with fuzzy soft set on TOPSIS.

### References

- [1] Zadeh LA. Fuzzy sets. *Inf Control*. 1965;8(3):338–353.
- [2] Arockiarani I, Lancy AA. Multi criteria decision making problem with soft expert set. *Int J Comput Appl*. 2013;78(15):15–22.
- [3] Atanassov K. Intuitionistic fuzzy sets. *Fuzzy Sets Syst*. 1986;20(1):87–96.
- [4] Saeed M, Sana A, Rubi N. Comparative study of airport evaluation problem by using fuzzy soft expert set and AHP technique. *Sci Int*. 2016;28(3):2439-2443.
- [5] Saeed M, Zulqarnain M. An application of interval valued fuzzy soft matrix in decision making. *Sci Int*. 2016;28(3):2261-2264.
- [6] Atanassov K. Operators over interval valued intuitionistic fuzzy sets. *Fuzzy Sets Syst*. 1994;64:159–174.
- [7] Gau Wl, Buehrer DJ. Vague sets. *IEEE Trans Syst Man Cybern*. 1993;23(2):610–614.

- [8] Gorzalcany MB. A method of inference in approximate reasoning based on interval-valued fuzzy sets. *Fuzzy Sets Syst.* 1987;21(1):1–17.
- [9] Maji PK, Biswas R, Roy AR. Fuzzy soft sets. *J Fuzzy Math.* 2001;9(3):589–602.
- [10] Maji PK, Biswas R, Roy AR. Soft set theory. *Comput Math Appl.* 2003;45(4-5):555–562.
- [11] Molodtsov D. Soft set theory-first results. *Comput Math Appl.* 1999;37(4-5):19–31.
- [12] Pawlak Z. Rough sets. *Int J Inf Comput Sci.* 1982;11(5):341–356.
- [13] Pawlak Z. *Hard set and soft sets, ICS research report.* Poland: Institute of Computer Science; 1994.
- [14] Prade H, Dubois D. *Fuzzy Sets and Systems: theory and applications.* London: Academic Press; 1980.
- [15] Zimmerman HJ. *Fuzzy Set Theory and its Applications.* Boston: Kluwer Academic Publishers; 1996.
- [16] Ramaseshan B, Yip LS, Pae JH. Power, satisfaction, and relationship commitment in Chinese store-tenant relationship and their impact on performance. *Journal of Retailing.* 2006;82(1):63–70.
- [17] Sanzo MJ, Santos ML, Vázquez R, Álvarez LI. The effect of market orientation on buyer-seller relationship satisfaction. *Industrial Marketing Management.* 2003;32(4):327–345.
- [18] Bruggen GH, Kacker M, Nieuwlaat C. The impact of channel function performance on buyer-seller relationships in marketing channels. *International Journal of research in Marketing.* 2005;22:141–158.
- [19] Yoon K, Hwang CL. *Multiple attribute decision making: methods and applications: a state-of-the-art survey.* Germany: Springer-Verlag; 1981.
- [20] Lai YJ, Liu TY, Hwang CL. TOPSIS for MODM. *Eur J Oper Res.* 1994;76:486–500.
- [21] Stern LW, El-Ansary AI, Coughlan AT. *Marketing Channels.* New Jersey: Prentice Hall; 1996.

## Exploration of Antibacterial Potential of *Melia Azedarach* L.

Munir, T.<sup>1\*</sup>, Mohyuddin, A.<sup>1</sup>, Khan, Z.<sup>2</sup> and Haq, R.<sup>3</sup>

<sup>1</sup>Department of Chemistry, University of Management and Technology

<sup>2</sup>Department of Botany, G. C. University Lahore,

<sup>3</sup>Department of Biotechnology, Lahore College for Woman University, Lahore.

\* mrs.waseemkhan@gmail.com,

### Abstract

*Melia azedarach* L. belongs to one of the most versatile medicinal plants family meliaceae (mahogany) which has great attraction for researchers. The plant was selected for research because it was one of the least explored members. The presence of saponin, alkaloids, tannins and flavonoids in the leaves extracts of plant indicated its medicinal value. These compounds have pharmacological effects against cancer, viral and malarial infections that are one of the main causes of deaths. With passage of time most of bacterial strains develop resistance against traditional medicines so they are needed to be upgraded or replaced. There is a need to develop antimicrobial agents with more effectiveness and minimum side effects. There are some reports from last two decades that *Melia azedarach* is a potential source of novel antibodies. Its extracts have both antioxidant and antimicrobial activities. Powdered leaves of *M. azedarach* were extracted with methanol and extract was preliminary examined by phytochemical tests and thin layer chromatography. The different concentrations of extracts showed good antibacterial activities against three pathogenic bacterial strains *Staphylococcus aureus*, *Escherichia coli* and *Bacillus thuringiensis*. The results indicated that *M. azedarach* L. could be an effective source of herbal medicines against infectious diseases.

**Keywords:** meliaceae, melia azedarach L, antibacterial activity.

### Introduction

The medicinal plants are major source of raw materials for treatment of various diseases in Ayurveda, Siddah and Unani traditional systems. In the modern medicine system the 25% of drugs are extracted from the plants. *Azadirachta indica* (former *Melia indica*) is widely used in herbal medicinal system. *Melia azedarach* L. (*M. azedarach*), although a close family relative, has been ignored in indigenous and modern system of medicine. The classification of two plants is presented in Table1 show their relevance with each other. The plant is native to Asia and is widely spread and naturalized in most of the subtropical and tropics parts of the world [1-4]. Deciduous tree of *M. azedarach* is small to medium in size. Maximum height is 15m and diameter is about 60cm. The plant has

characteristic dark green dense and spreading crowned with dark brown bark. Dark green, pale leaves are short stalked, hairless and thin and white flowers having purple stripes and fragrance ( 1, 2). It has yellow round, smooth and fleshy berries with four to five seeds [5].

Table1.

Classification of *M. azedarach* and *A. indica*

Category	<i>Melia azedarach</i> L. ( <i>dhraik</i> )	<i>Azadirachta Indica</i> (neem)
Kingdom	Plantae	Plantae
Bionomial Name	<i>Melia azedarach</i> L.	<i>Azadirachta Indica</i>
Division	Magnoliophyta	Magnoliophyta
Class	Magnoliopsida	Magnoliopsida
Order	Sapindales	Sapindales
Family	Maliaceae	Maliaceae
Genus	<i>Melia</i>	<i>Azadirachta</i>
Species	<i>M.azedarach</i>	<i>M.Indica</i>
Synonyms	<i>Melia australis sweet</i>	<i>Melia indica</i>

The extracts of leaves, fruits have antioxidant, analgesic and antimicrobial activities. The plants also showed antifungal, antimalarial & cytotoxic activities. Alkaloids, flavonoids, glycosides, saponins & tannins present in the methanolic extract of plant [5]. It has been used as a bitter tonic, fuel, an anthelmintic, astringent and an antiseptic agent [6]. It has been shown curing properties for diseases such as rheumatism, leprosy, rashes etc [7]. It is revealed from a literature survey that limonoides, limonin, nomilin and obacunone have been discovered [8]. The oil of *M. azedarach* contains sulfur containing limonoids which has been used in soap & cosmetic industries [9].

Figure1. Leaves of *Melia Azedarach* LinnFigure2. Flowers of *Melia Azedarach* Linn

## 2. Materials

### 2.1. Collection and Identification of Plant Material

The plant material of *M. azedarach* L. was collected from garden of G.C. University of Lahore. Taxonomist Prof. Dr. Zaheer-Ud-Din Khan of Govt. College University Lahore identified the plants. Further the plant specimen was deposited at herbarium of G.C University.

Family : *Meliaceae*

Species : *Melia Azedarach* Linn.

Voucher No.: G.C. Herb Bot. 2908

### 2.2. Drying Of Plant Material

The fresh plants leaves were placed in clean stainless tray and kept under shade at temperature of 20°C to 25°C for one week. After drying the leaves were powdered by mechanical means.

## 3. Methodology

### 3.1. Soxhlet Extraction

An average of 40g (500g total) of dried and powdered plant leaves were taken at a time in the thimble and put into the Soxhlet apparatus. Plant material was extracted with 350ml of methanol for 4 to 6 hours. The crude extract obtained was filtered with filter paper and the filtrate was then analyzed further. The extract was concentrated in a rotary evaporator for complete removal of methanol [7].

### 3.2. Detection of Secondary Metabolites in Crude Plant Extract

For detection of secondary metabolites, 4g of powdered plant leaves were extracted with methanol (50ml), boiled it for 5 minutes, cooled and filtered. In the filtrate added small amount of Lead acetate to make solution. Filtered and divided in several parts. Different tests were applied for the Tannins, Flavonoids, Alkaloids and Saponins according to standard procedures [10].

### 3.3. Thin Layer Chromatography

The TLC was carried out with BAW (Butanol, Acetic Acid CH<sub>3</sub>COOH, H<sub>2</sub>O in ratio 4:1:5) as solvent. After drying, the chromatogram was observed under UV lamp. The wave length 366 nm was used for observation. Distribution of components was good and different colored spots were observed. Pattern of colored spots was recorded and R<sub>f</sub> value of each spot was calculated.

### 3.4. Antibacterial activity

The antibacterial investigation was carried out by well diffusion method against three pathogenic bacterial strains. *Bacillus thuringiensis* (Ref. # BL- Bt6), *Staphylococcus aureus* (ATCC # 6633) and *Escherichia coli* (ATCC # 25922). The concentrated methanolic extract of leaves of *M. azedarach* L was dissolved in distilled water and different concentrations were prepared.

Nutrient broth was dissolved in distilled water and heated. Adjust the PH to 7.4 and then sterilized it in an autoclave for 25 minutes. Added some agar in it and heated again. Bacterial cultures were taken from stock slants. The bacterial cultures were incubated at 37°C for one day. These cultures were then added to conical flask which consists of freshly prepared nutrient broth and placed in a shaker at 37°C and incubated for one day. The nutrient agar in molten form was poured as a basal layer in petri dishes. Plates were inoculated with respective organism. After solidification, wells were bore which were then fill with control and extracts of different concentrations, and incubated again for 24 hours at 37 °C. The diameters of zones of inhibition around the wells were recorded. The antibacterial activity of plant extracts were estimated by evaluation of Minimum inhibitory concentration (MIC) [11-13].

## 4. Results and Discussions

### 4.1. Phytochemical Analysis

Phytochemical analysis of *M. azedarach* methanol leaves extracts was carried out to investigate the absence or presence of alkaloids, flavonoids, saponins, glycosides and tannins in leaves and the results are presented in the Table2. The results supported the previous studies that plant contained Alkaloids, Tannins, Steroids Saponins [14].

Test results revealed that plant leaves contain bioactive compounds like Alkaloids, Steroids, Saponins, Tannins, and flavonoids. These compounds are responsible for the antimicrobial efficacy of plant. However the sample extract did not show the presence of Anthraquinones.

Table2.

Phytochemical analysis of methanolic extract of leaves

Experiment Test for Alkaloids:	Observation	Inference
Mayer's test	Yellow ppt.	Alkaloid present
Wagner's test	Reddish Brown ppt.	Alkaloid present
Hagner's test	Yellow ppt.	Alkaloid present
Dragendorff test	Cloudy Appearance	Alkaloid present
<b>Test for Tannins:</b>		

5ml extract + 6 drop FeCl <sub>3</sub> and allowed to stand for 5 minutes	Bluish Green ppt.	Tannins present
<b>Test for Flavonoids:</b>		
Plant extracts+2 ml AlCl <sub>3</sub> .	Yellow Fluorescence	Flavonoids present
<b>Test for Steroids:</b>		
Leiberman-Burchard test	Violet Color	Steroids present
<b>Test for Saponnins:</b>		
Shook the aqueous plant vigorously	Persistent Froth	Saponnins present
<b>Test for Anthraquinones:</b>		
Plant extract + few drops of <i>N</i> , <i>N</i> -dimethyleaniline	No red color	Anthraquinones absent

#### 4.2. Thin Layer Chromatography

TLC on prepared TLC card (0.2 mm) was used for the initial investigation of bioactive compounds present in methanolic leaves extracts of *M. azedarach*. The chromatogram showed three differently colored spots under UV lamp (Table3). The R<sub>f</sub> values of spots were compared with the standard data from Harborne [15] for general indication of classes of compounds present. The R<sub>f</sub> values indicated the existence of Anthocyanidin-3-glycosides, Anthocyanidin 3, 5–diglycosides or isoquercetin and rutinosides.

Table3.

TLC of the methanolic extract using BAW

No. of spot	Color in UV light (366nm)	R <sub>f</sub> value	Expected compounds
1	Orange	0.674	Anthocyanidin-3-glycosides
2	Red	0.584	Anthocyanidin 3,5–diglycosides or isoquercetin
3	Green	0.426	Rutinosides

#### 4.4. Antibacterial Activity

*M. azedarach* L was reported to have antibacterial properties against bacterial strains other than those used in this study [16,17]. The antibacterial activity of *M. azedarach* L was investigated by using three concentrations of concentrated methanolic leaves extract in methanol as 100 mg/ml (D2), 50 mg/ml (D2), and 10 mg/ml (D1). Control used was Streptomycin for whom average diameter of zone of inhibition was 27.5mm. The extracts showed significant inhibition against Gram positive as well as Gram negative bacteria as shown in Table4.

The maximum inhibition was observed by concentration D1 in case of *Escherichia coli* while *Bacillus THURINGIENSIS* AND *Staphylococcus aureus* gave maximum reduction on concentration D2. This indicated the different response of Gram positive and Gram negative bacteria against bioactive compounds.

Table4.

Antibacterial activity of *M. azedarach* leaves extract

Bacterial Strain	Type of Bacteria	Diameter of zone of inhibition(mm)			
		Methanol	D1 <sup>a</sup>	D2 <sup>b</sup>	D3 <sup>c</sup>
<i>Bacillus thuringiensis</i>	Gram positive	0	27	28	11
<i>Staphylococcus aureus</i>	Gram positive	0	27	31	17
<i>Escherichia coli</i>	Gram negative	0	39	32	12

<sup>a</sup> D1 showed concentration 100 mg/ml

<sup>b</sup> D2 showed concentration 50 mg/ml

<sup>c</sup> D3 showed concentration 50 mg/ml

A Comparison of MIC value of three bacteria is demonstrated in Figure3. It showed that methanolic extract of *M. azedarach* is most potent against *Staphylococcus aureus*. Therefore in view of previous reports and present study, *M. azedarach* was found to be much potent and having bioactive compounds [18-21].

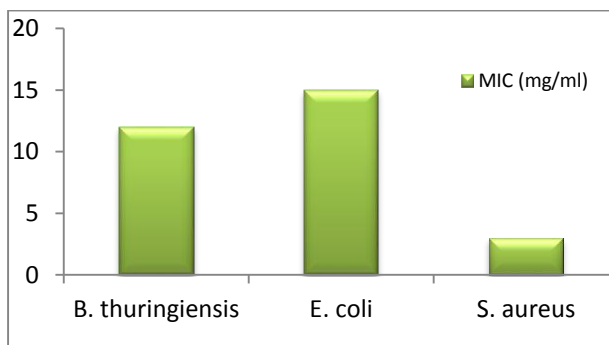


Figure3. Comparison of MIC of three bacteria

## 5. Conclusion

The *M. azedarach* is famous for its important alkaloid content. Phytochemical tests and TLC showed that the plant leaves extract contains large variety of secondary metabolites such as alkaloids, flavonoids, saponins, tannins and glycosides. Due to presence of such compounds, the plant exhibited significant antimicrobial activity against pathogenic bacteria. The leaves extract of plant showed high antibacterial potential and gave significant zones of

inhibition. The study indicated that *M. azedarach* can contribute well in the herbal medicinal system so it can be concluded that there is a need to explore and accept its medicinal value. The bioactivity spectrum of plant against pathogenic bacteria is worth noticing. Since the bioactive compounds present in the leaves extract of plant are responsible for the significant antimicrobial activity against the tested microorganisms so this plant need to be explored further for its medical potency.

### References

- [1] Mishra M, Jawla S, Srivastava V. Melia Azedarach: a review. *Int J Med Chem Anal.* 2013;3(2):53–56.
- [2] Ramya S, Jepachanderamohan PJ, Alaguchamy N, Kalayanasundaram M, Jayakumararaj R. In vitro antibacterial prospective of crude leaf extracts of *Melia azedarach* Linn. against selected bacterial strains. *Ethnobotanical Leaflets.* 2009;13(10):254–58.
- [3] Sharma D, Paul Y, Preliminary and pharmacological profile of *Melia azedarach* L.: an overview. *J Appl Pharm Sci.* 2013;3(12):133–138.
- [4] Xiao J, Zhang Q, Gaoa U, Shib X, Gaoa JM. Antifungal and antibacterial metabolites from an endophytic *Aspergillus sp.* associated with *Melia azedarach*. *Nat Prod Res.* 2014;28(17):1388–1392.
- [5] Azam MM, Mamun-or-Rashid AN, Towfique N.M, Sen MK, Nasrin S. Pharmacological potentials of *Melia azedarach* L - a review. *Am J Biosci.* 2013;1(2):44–49.
- [6] Kaneria, BY, Vaghasiya Y, Chanda S. Determination of antibacterial and antioxidant potential of some medicinal plants from Surashtra region India. *Indian J Pharm Sci.* 2009;71(4):406–412.
- [7] Sen A, Batra A. Evaluation of antimicrobial activity of different solvents extracts of medicinal plants: *Melia azedarach* Linn. *Int J Curr Pharm Res.* 2012;4(2):67-73.
- [8] Neeycee MA, Nematzadeh GH, Dehestani A, Alavi M. Evaluation of antibacterial effects of chinaberry (*Melia azedarach*) against gram-positive and gram-negative bacteria. *Int J Agric Crop Sci.* 2012;4(11):709–712.
- [9] Deepika S, Yash P. Preliminary and pharmacological profile of *Melia azedarach* L.: an overview. *J Appl Pharm Sci.* 2013;3(12):133–138.

- [10] Asadujjaman M, Saed A, Aslam HM, Utpal K. Assessment of bioactivities of ethanolic extract of *Melia azedarach* (Meliaceae) leaves. *J Coastal Life Med.* 2013;1(2):118–122.
- [11] Marimuthu S, Balakrishnan P, Nair S. Phytochemical investigation and radical scavenging activities of *Melia azedarach* and its DNA protective effect in cultured lymphocytes. *Pharm Biol.* 2013;51(10):1331–40.
- [12] Khatoon A, Jethi S, Nayah SK, Sahoo S, Mohapatra A, Satapathy K. Evaluation of in vitro antibacterial and antioxidant activities of *Melia azedarach* L. bark. *IOSR J Pharm Biol Sci.* 2014;9(6):14–17.
- [13] Paritala V, Chiruvella KK, Thammineni C, Ghanta RG, Mohammad A. Phytochemical and antimicrobial potential of mahogany family. *Rev Bras Farmacogn.* 2015;25(1):61–83.
- [14] Zhang WM, Liu JQ, Peng XR, Wan LS, Zhang ZR, Li ZR, et al. Triterpenoids and sterols from the leaves and Twigs of *Melia Azedarach*. *Nat Prod Bioprospect.* 2014;4(3):157–162.
- [15] Harborne JB. *Phytochemical Methods*. London: Chapman and Hall; 1974.
- [16] Khan N, Abbsi AM, Dastagir G, Nazir A, Shah GM, Shah MM, et al. Ethnobotanical and antimicrobial study of selected medicinal plants used in khyber pakhtunkhwa as a potential sources to cure infectious diseases. *BMC Complementary Altern Med.* 2014;14:122.
- [17] Hossain MA, Saud M, Majeed. Study of the Antimicrobial effect of *Melia azedarach* Linn. *Journal of the Biotechnology of Research.* 2013;7:1.
- [18] Rupa BA, Azam MN, Mannan MA, Ahmed MN, Hassan MN. Photochemistry and pharmacological appraisals of Persian Lilac (*Melia azedarach* Linn.): A quick comprehensive review. *American Journal of Ethnomedicine.* 2014;1:152–163.
- [19] Adnan Y, AL-Rubae. The Potential uses of *Melia azedarach* L. as pesticidal and medicinal plant. *Am-Eurasian J Sustain Agric* 2009;3(2):185–194.
- [20] Sultana S, Akhtar N, Asif HA. Phytochemical screening and antipyretic effects of hydro-methanol extract of *Melia azedarach* leaves in rabbits. *Bangladesh J Pharmacol.* 2013;8(2): 214–217.
- [21] Khan MR, Kihara M, Omoloso AD. Antimicrobial activity of *Horsfieldia helwigii* and *Melia azedarach*. *Fitoterapia.* 2001;72(4):423–7.

## DFT-Mbj Study of Electronic and Magnetic Properties of Cubic $\text{CeCrO}_3$ Compound: An Ab-Initio Investigation

Rashid, M<sup>1.</sup>, Iqbal, M. A<sup>2.</sup> and Noor, N. A<sup>3\*</sup>.

<sup>1</sup>Department of Physics, COMSATS Institute of Information Technology, Islamabad, Pakistan

<sup>2</sup>Department of Physics, University of Management and Technology, Lahore, Pakistan

\*naveedcssp@gmail.com

### Abstract

*By considering density functional theory (DFT) in terms of ab-initio investigation, we have explored the structural, electronic and magnetic properties of cubic  $\text{CeCrO}_3$  for the first time. In order to determine the structural stability of cubic  $\text{CeCrO}_3$  compound, we optimized the structure of  $\text{CeCrO}_3$  in non-magnetic (NM), ferromagnetic (FM) and Anti-ferromagnetic (AFM) phases by using PBE generalized gradient approximation (GGA) functional to find the exchange-correlation potential. From structural optimization, the FM phase of  $\text{CeCrO}_3$  is observed to be stable. For computing electronic and magnetic properties, the lately advanced modified Becke and Johnson local (spin) density approximation (mBJLDA) is used. Calculated band structures and density of states plots with an integer magnetic moment of  $4 \mu_B$  and reveal half-metallic character. In addition,  $s$ - $d$  exchange constants ( $N_0\alpha$ ) and  $p$ - $d$  exchange constant ( $N_0\beta$ ) are determined, which are in agreement with a distinctive magneto-optical experiment.*

**Keywords:** *ab-initio calculations, cubic perovskite, half-metallic ferromagnetic, magnetic properties*

### Introduction

Magneto-electric (ME) characteristic in the multi-ferroics, now a day's has become of vigorous importance, due to the existence of correlated ordering parameter of electric and magnetic components that gets so much attention for famous existing application such as sensor of magnetic field, memory elements for multiple state, spintronic and multi-range microwave devices etc [1-3]. Detail information of crystal and magnetic structure is matter of great concern for useful application. Recently, the rare-earth ortho-ferrites have been reported like  $\text{GdFeO}_3$  [5] and  $\text{DyFeO}_3$  [4] have been reported for ferro-electricity as well as ME coupling effects. It is very difficult to perform polarization measurement caused by high leakage current due to high Neel temperature of  $\text{RFeO}_3$  ( $T_N^{\text{Fe}}=620-740\text{K}$ ). At the same time as perovskite chromite  $\text{RCrO}_3$  exhibits magnetic properties at lower TN values (110–280K).  $\text{RCrO}_3$  (R=Sm- Gd- Tb- Er- Tm- and Y) [6,7] was reported to show signs of a fairly great electric polarization

( $0.2\text{--}0.8\mu\text{C}/\text{cm}^2$ ), initially, at somewhat high temperatures equivalent to the  $T_N$  of the Cr sub-system. Additionally,  $\text{LaCrO}_3$ ,  $\text{CeCrO}_3$  have the maximum  $T_N$  in  $\text{RCrO}_3$  compounds, which is advantageous for device applications at room temperature [8].

Perovskite oxides get so much attention due to its effective use in gas separation membranes, solid fuel cell and piezoelectric etc. [9-14]. Lanthanide doped perovskite type oxides, for example  $\text{LnMeO}_3$  (Ln: lanthanides, Me: transition metals), have been accustomed for functional inorganic materials having a inclusive diversity of applications for alkaline fuel cells electrodes [15], gas ions sensors [16] and catalysts for fast and complete oxidation/reduction of CO, NO and other hydrocarbons [17]. Various fascinating physical properties such as structural, electronic, optical and magnetic properties are inter-dependent in transition-metal oxides [18, 19]. These materials are predictable for spintronics devices effectively.

The association of magnetic and electronic played a role to develop the research in area of spintronics. Half-metallic ferromagnetism has a significant part because of its spin- polarization at the Fermi-level which is necessary for the better performance of spintronic applications [20, 21]. All these points force us to explore half-metallic ferromagnets with important magnetic moment that well-matched with existing semiconductor technology. Material similar to half-metal have a unique property to act as conductor in one direction of spin and insulator for opposite direction, therefore, it is very suitable for device applications and get attention for researcher that are working in the area of spintronic devices [22-24]. Some major examples are magnetic disk drives, magnetic tunnel junctions, magnetic hybrid technology for CMOS and magnetic sensor [25, 26], non-volatile magnetic random access memories (MRAM) [27, 28]. By getting research inspiration from de Groot et al. work, that explicate the insight of half-metallicity to compute band structure using the half-Heusler alloys  $\text{NiMnSb}$  [29]. Several research groups perform numerous experimental and computational studies on the HM ferromagnets, and many HM materials have been predicted and experimental verified [30].

$\text{CeCrO}_3$  belongs to Pm-3m (No. 221) space group and have cubic crystal structure. The atoms arrangement are as that Cr ions are placed at center of unit cell and coordinated with 6 oxygen ions, Ce ions are distributed at the corner of the cell and oxygen at center of the faces of unit cell. We have applied mBJ scheme, as introduced by Becker and Johnson (BJ) [31], as it can properly find electronic and magnetic characteristics. The structural properties of aforesaid crystals are calculated at ground state and equated with the prevalent theoretical and experimental data.

## 2. Method of Calculations

In this study, predicted results were obtained by carrying the Density Functional Theory (DFT), which is quantum mechanical approach that successful in predicting fundamental properties of compounds and alloys in terms of semiconducting trend. We employed DFT based full potential linearized augmented plane wave plus local orbital (FP-LAPW+lo) method within the framework of Wien2K code [32]. In order to determine the ground state factors like lattice constant and bulk modulus, we used generalized gradient approximation (GGA) functional by considering the exchange-correlation potential suggested by Perdew, Burke, and Ernzerhof (PBE) [33]. Whereas, recently developed modified Becke-Johnson local density approximation functional (mBJLDA) [31] were used to analyze the magnetic and electronic properties. The aim of using mBJLDA potential for electronic properties is because of that exploring the improved predicting bandgap as associated with standard LDA [34] or GGA [33].

In FP-LAPW+lo method, ion cores inside non-overlapping spheres and a region of constant potential (interstitial region) are considered to the region between the spheres. In interstitial region, a plane wave expansion is used, whereas basis functions, potential and charge density were prolonged as arrangements of spherical harmonic functions. The value of  $l_{max}=10$  in muffin-tin spheres for charge density and non-spherical potential was accomplished. For energy merging, basis function expand upto  $R_{MT} \times K_{max} = 8$  (in the plane wave extension  $R_{MT}$  represent the minimum sphere radius and  $K_{MAX}$  the amount of the largest K vector). A mesh of 56 k-points was used in the irreducible part of the Brillouin zone (BZ) for structural, magnetic and electronic properties, which certifies the convergence, are 3000 k-points. In addition, the charge density was Fourier prolonged up to  $G_{max} = 16$ . For cubic  $CeCrO_3$  perovskites, the  $R_{MT}$  values were elected to be 2.5, 1.72 and 1.87a.u. (atomic units) for Ce, Cr and O correspondingly. For energy convergence, the calculations of self-consistent were performed iteratively, when the total energy of the system is steady within 0.01 mRy.

## 3. Results and Discussion

### 3.1. Structural properties

To understand DFT based cubic  $CeCrO_3$ , structure stability is check by performing structural optimization in NM, FM and AFM phases. By using GGA-PBE scheme, optimization is done by minimizing the total energy with reverence to unit cell volume in each phase. From computed results (see Figure1), the total energy difference between these two as  $\Delta E = E_{NM} - E_{FM}$  and  $\Delta E = E_{AFM} - E_{FM}$ . The positive of  $\Delta E$  confirmed that  $CeCrO_3$  is stable in FM phase (see Table 1). In  $ABO_3$  oxides with B=Mn, Cr, Fe, Ni and Co, most of such oxides have FM

character. Similar, FM character is also proved in our study. Therefore, in first step, we performed optimization in FM phase to compute the lattice constant  $a(\text{\AA})$  and bulk modulus  $B$  for  $\text{CeCrO}_3$  are shown in Table1.

The calculated tolerance factors for  $\text{CeCrO}_3$  are mentioned in Table1. Our calculated value of tolerance factor is in adjacent covenant with the calculated results [35, 36]. In cubic perovskite, the tolerance factor lies between 0.93 and 1.02 [36] and our measured values employed in this range, illuminating the cubic structure of  $\text{CeCrO}_3$  compounds. The bond lengths are measured between various atoms of the  $\text{CeCrO}_3$  and also listed in Table1. The tolerance factor can be calculated using bond lengths by using the consequent formula:

$$t = \frac{0.707(\langle Ce - O \rangle)}{\langle Cr - O \rangle}$$

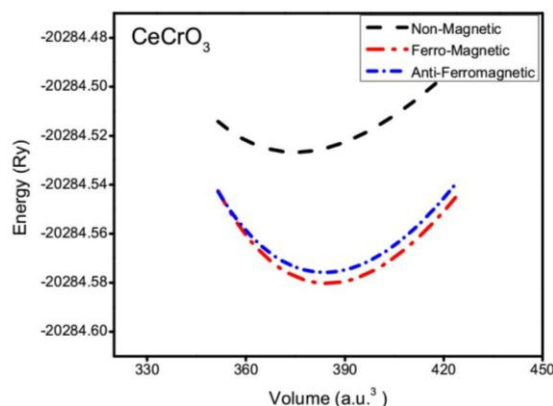


Figure1. The computed total minimum energy versus unit cell volume in non-magnetic, ferro-magnetic and anti-ferromagnetic cubic  $\text{CeCrO}_3$  compound

Table1.

Calculated lattice parameters  $a(\text{\AA})$ , Bulk moduli  $B(\text{GPa})$ , Tolerance factor, Bond length, bandgap  $E_g$  (eV), Half-metallic  $E_{HM}$ (eV), magnetic moments ( $\mu_B$ ) and exchange constant parameters of FM cubic  $\text{CeCrO}_3$

Parameter	$\text{CeCrO}_3$
$a_0(\text{\AA})$	3.877
$B_0(\text{GPa})$	183.81
Tolerance factor	0.999
Bond length Cr-O	1.9373
Bond length Ce-O	2.7397
Bond length Cr-Ce	3.355
$E_g$ (eV)	2.89
$E_{HM}$ (eV)	0.38

Total ( $\mu_B$ )	4.0004
Cr ( $\mu_B$ )	2.5283
Ce ( $\mu_B$ )	0.9831
O ( $\mu_B$ )	0.0642
$\Delta x$ (d)	4.25
$\Delta x$ (pd)	3.14
$\Delta E_C$ (eV)	0.42
$\Delta E_v$ (eV)	2.70
$N_{o\alpha}$	0.33
$N_{o\beta}$	2.14

### 3.2. Electronic properties

Electronic band structure with mBJ DFT studies was discussed in this electronic part. Energy eigen values obtained with the help of KS equation for Electronic band structure. In the magnetic properties of  $CeCrO_3$  show match of band structure due to spin up ( $\uparrow$ ) and down ( $\downarrow$ ) orientation of FM  $CeCrO_3$  polarized band structure in Figure2. In the analysis of spin-up state band structure, it will be seen that the valance band (VB) maxima and conduction band (CB) minima both found at point M of Brillion Zone (see in Figure2). For above analysis, it is seen that up spin state of  $CeCrO_3$  demonstrate the FM semiconductors behavior. The VB maxima cross the Fermi level ( $E_F$ ) for spin down channel in  $CeCrO_3$ , which describe the half-metallic manners is there for spin down ( $\downarrow$ ) state. To disclose the starting point of density of states, partial density of state for  $CeCrO_3$  is calculated and shown in the Figure3.

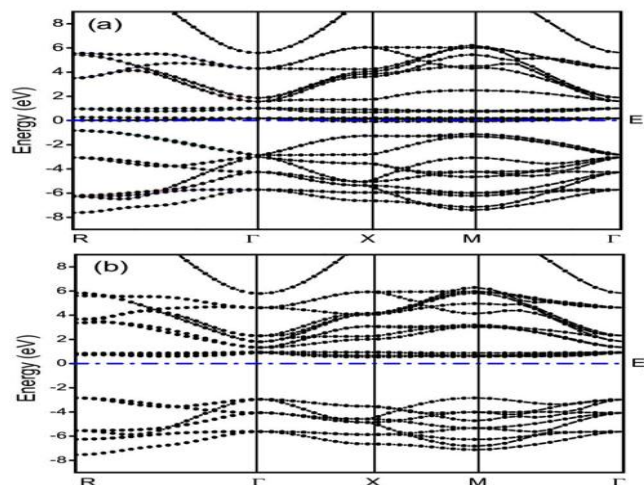


Figure2. The Calculated Spin Polarized Ferromagnetic Band Structures for Cubic  $CeCrO_3$  Compound with Mbj Potential

The (a) for majority spin ( $\uparrow$ ) and the (b) for minority spin ( $\downarrow$ )

It understood able the Fermi level  $E_F$  is cross for spin up, total DOS, on the other hand the down channel form band gap at  $E_F$ , resultant the charges make a complete spin polarization and form this compound to utilize it for spintronics devices. For compound  $\text{CeCrO}_3$  and by means of mBJ  $2p$  states and  $3d$  states of O and Cr contributed primarily in the region of VB involving  $-4$  eV to Fermi level. If we deeply analyzed DOS from  $E_F$  to  $1$  eV, we observed the  $4f$  orbitals of Ce contribution in DOS, after active over  $3d$  states of Cr is clearly depicted. The shift in these states to-wards high energies and the contribution of  $4f$  states of Ce increments in the region of Fermi level clues to observed p-type conductivity and 100% spin polarization.

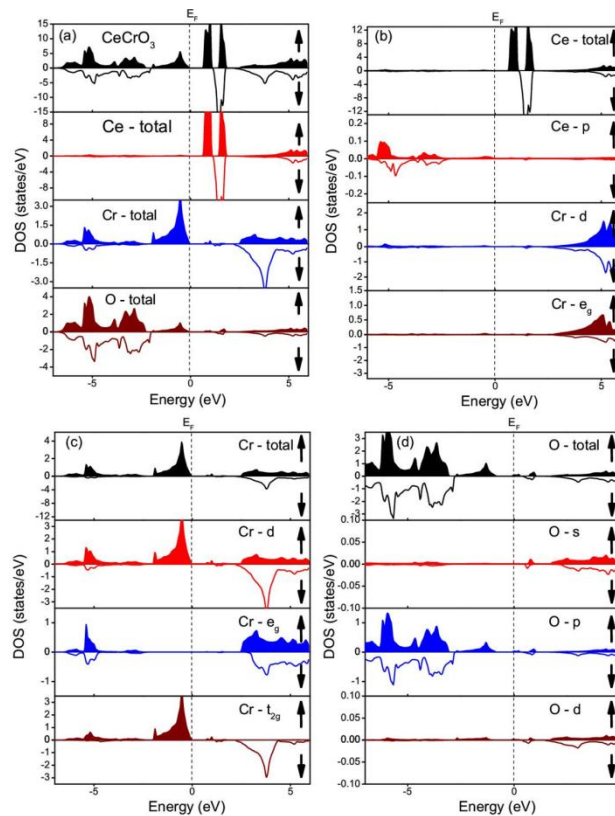


Figure3. The calculated (a) total density of states (DOS), along partial DOS of (b) Ce, (c) Cr and (d) O by using mBJ for  $\text{CeCrO}_3$  compound.

### 3.3. Magnetic Properties

We obtained magnetic moment  $\text{CeCrO}_3$  from mBJ and listed in the Table1. Although, the calculated value is to some extent lesser than the theory value ( $\mu_{\text{Cr}}=2.52 \mu\text{B}$ ). The fact of the smaller value is that the electrons in  $3d$  are

not totally confined but hybridized with oxygen of its  $2p$  states. We have been also calculated magnetic moments of Ce ions. From the calculation we suggest that the total magnetic moment is predominantly because of Cr atoms and the  $M_{Ce}$  may be negligible. The half metallic characteristic of materials is verified by the numeral value of total magnetic moment. In our verdict the dual exchange method is liable for ferromagnetism seen in  $CeCrO_3$  cubic perovskites and has indirect exchange interface among transition metals and rare-earths by the mean of anion O.

In addition splitting energy  $\Delta_x(d)$  values of spin exchange that describes the role of  $3d$  states of transition metal in exchange method is studied for Cr, and listed in the Table1. Most exciting calculated parameters from  $p-d$  and  $s-d$  coupling are swap coefficients  $N_{0\alpha}$ ,  $N_{0\beta}$ , correspondingly [37], that decide the swap interaction among TM  $d$ -state as well as charge carriers (holes and electrons in the valance band and conduction band respectively). The swap coefficients values for  $CeCrO_3$  are shown in Table1. Additional, the value of  $N_{0\alpha}$  has lower than  $N_{0\beta}$  indicate that the  $s-d$  contact at CB minima is greatly feebler than  $p-d$  interaction at VB maxima, that may be evidence of ferromagnetic behavior present in the given compound.

#### 4. Conclusion

In conclusion, we have perceived structural, electronic and magnetic properties of FM  $CeCrO_3$  compound by means of ab-initio calculations. To verify the stability of  $CeCrO_3$  compound, we have optimized the structure in PM, FM and AFM phases and have computed their total energy differences ( $\Delta E_1$  and  $\Delta E_2$ ). The calculated value of  $\Delta E_1$  and  $\Delta E_2$  are positive, which confirm that  $CeCrO_3$  is stable in FM phase. By analyzing band structure and density of state plots, we find that  $CeCrO_3$  is a half-metallic ferromagnet, while predicted value of total magnetic moments is  $4 \mu_B$ . In addition, Cr  $3d$  (unfilled) state due to  $p-d$  hybridization results in a fall of magnetic moment of Cr ions and identical of magnetic moment in the Ce and O (nonmagnetic) ions. Furthermore, calculated exchange constant  $N_{0\alpha}$  and  $N_{0\beta}$  indicate a lower value of  $N_{0\alpha}$  than  $N_{0\beta}$ , which represents that spin-down state is more operative, due to  $p-d$  interaction at valance band maxima and ferromagnetism is confirmed by their strong hybridization. Furthermore, double-exchange mechanism is used to discuss the origin of the ferromagnetism in  $CeCrO_3$ .

### References

- [1] Spaldin NA, Fiebig M. The renaissance of magnetoelectric multiferroics. *Science*. 2005;309(5733):391–392.
- [2] Fiebig M. Revival of the magnetoelectric effect. *J Phys D Appl Phys*. 2005;38(8):123–152.
- [3] Khomskii D. Classifying multiferroics: mechanisms and effects. *Physics*. 2009;2(20):20–28.
- [4] Tokunaga Y, Iguchi S, Arima T, Tokura Y. Magnetic-Field-Induced Ferroelectric State in DyFeO<sub>3</sub>. *Phys Rev Lett*. 2008;101(9):097205–097210.
- [5] Tokunaga Y, Furukawa N, Sakai H, Taguchi Y, Arima TH, Tokura Y. Composite domain walls in a multiferroic perovskite ferrite. *Nat Mater*. 2009;8:558–562.
- [6] Rajeswaran B, Khomskii DI, Zvezdin AK, Rao, CN, Sundaresan A. Field-induced polar order at the Néel temperature of chromium in rare-earth orthochromites: Interplay of rare-earth and Cr magnetism. *Phys Rev B*. 2012;86(21):214409–214415.
- [7] Serrao CR, Kundu AK, Krupanidhi SB, Waghmare UV, Rao CN. Biferroic YCrO<sub>3</sub>. *Phys Rev*. 2005;B72:220101–220108.
- [8] Zhou JS, Alonso JA, Pomjakushin V, Goodenough, JB, Ren Y, Yan JQ, et al. Intrinsic structural distortion and super exchange interaction in the orthorhombic rare-earth perovskites RCrO<sub>3</sub>. *Phys Rev B*. 2010;81(21):214115–214120.
- [9] Fong DD, Stephenson GB, Streiffer SK, Eastman JA, Auciello O, Fuoss PH, et al. Ferroelectricity in ultrathin perovskite films. *Science*. 2004;304(5677):1650–1653.
- [10] Petric A, Huang P, Tietz F, Evaluation of La–Sr–Co–Fe–O perovskites for solid oxide fuel cells and gas separation membranes. *Sol State Ion*. 2000;135(1–4):719–725.
- [11] Pena MA, Fierro JL. Chemical Structures and performance of Perovskite Oxide. *Chem Rev*. 2000;101(7):1981–2017.
- [12] Galasso FS. *Perovskites and High Tc Superconductors*. New York: Gordon and Breach; 1990.
- [13] Murtaza G, Ahmad I, Amin B, Afaq A, Maqbool M, Maqsood JK, et al. Investigation of structural and optoelectronic properties of BaThO<sub>3</sub>. *Opt Mater*. 2011;33(3):553–557.
- [14] Hayatullah, Murtaza G, Khenata R, Mohammad S, Naeem S, Khalid MN, et al. Structural, elastic, electronic and optical properties of CsMCl<sub>3</sub> (M=Zn, Cd). *Physica B*. 2013;420:15–23.

- [15] Meadowcroft DB. Low-cost oxygen electrode material. *Nature*. 1970;226:847–848.
- [16] Yang M, Huo L, Zhao H, Gao S, Rong Z. Electrical properties and Acetone-Sensing characteristics of  $\text{LaNi}_{1-x}\text{Ti}_x\text{O}_3$  Perovskite System Prepared by Amorphous Citrate Decomposition. *Sens Actuators B Chem*. 2009;143(1):111–118.
- [17] Zhang HM, Shimizu Y, Teraoka Y, Miura N, Yamazoe N, Oxygen sorption and catalytic properties of  $\text{La}_{1-x}\text{Sr}_x\text{Co}_{1-y}\text{Fe}_y\text{O}_3$  Perovskite-type oxides. *J Catal*. 1990;121(2):432–440.
- [18] Wong KM, Alay-e-Abbas SM, Shaukat A, Fang Y, Lei Y. First-principles investigation of the size-dependent structural stability and electronic properties of O-vacancies at the ZnO polar and non-polar surfaces. *J Appl Phys*. 2013;113(1):014304.
- [19] Wong KM, Alay-e-Abbas SM, Fang Y, Shaukat A, Lei Y. Spatial distribution of neutral oxygen vacancies on ZnO nanowire surfaces: an investigation combining confocal microscopy and first principles calculations. *J Appl Phys*. 2013;114(3):034901.
- [20] Wolf SA, Awschalom DD, Buhrman RA, Daughton JM, von-Molnar S, Roukes ML, et al. Spintronics: a spin-based electronics vision for the future. *Science*. 2001;294(5546):1488–95.
- [21] Pickett WE, Moodera JS. Half metallic magnets. *Phys Today*. 2001;54:39.
- [22] Saeed Y, Nazir S, Shaukat A, Reshak AH. Ab-initio calculations of Co-based diluted magnetic semiconductors  $\text{Cd}_{1-x}\text{Co}_x\text{X}$  (X=S, Se, Te). *J Magn Magn Mater*. 2010;322(20):3214–3222.
- [23] Nazir S, Ikram N, Siddiqi SA, Saeed Y, Shaukat A, Reshak AH. First principles density functional calculations of half-metallic ferromagnetism in  $\text{Zn}_{1-x}\text{Cr}_x\text{S}$  and  $\text{Cd}_{1-x}\text{Cr}_x\text{S}$ . *Curr Opin Solid State Mater Sci*. 2010;14(1):1–6.
- [24] Saini HS, Singh M, Reshak AH, Kashyap MK. Emergence of half metallicity in Cr-doped GaP dilute magnetic semiconductor compound within solubility limit. *J Alloy Compd*. 2012;536:214–218.
- [25] Wurmehl S, Fecher GH, Kandpal HC, Ksenofontov V, Felser C, Lin HJ. Investigation of  $\text{Co}_2\text{FeSi}$ : the Heusler compound with highest Curie temperature and magnetic moment. *Appl Phys Lett*. 2006;88(3):032503.
- [26] Wang W, Liu E, Kodzuka M, Sukegawa H, Wojcik M, Jedryka E, et al. Coherent tunneling and giant tunneling magnetoresistance in  $\text{Co}_2\text{FeAl}/\text{MgO}/\text{CoFe}$  magnetic tunneling junctions. *Phys Rev B*. 2010;81(14):140402.

- [27] Zutic I, Fabian J, Das-Sarma S. Spintronics: fundamentals and applications. *Rev Mod Phys.* 2004;76(2):323.
- [28] Karaca M, Kervan S, Kervan N. Half-metallic ferromagnetism in the CsSe compound by density functional theory. *J Alloy Compd.* 2015;639:162–167.
- [29] de Groot RA, Mueller FM, van Engen PD, Buschow KH. New Class of Materials: Half-Metallic Ferromagnets. *Phys Rev Lett.* 1983;50(25):2024.
- [30] Si C, Zhou J, Sun Z, Half-Metallic ferromagnetism and surface functionalization-induced metal–insulator Transition in Graphene-like two-dimensional Cr<sub>2</sub>C crystals. *ACS Appl Mater Interfaces.* 2015;7(31):17510–17515.
- [31] Tran F, Blaha P. Accurate band gaps of semiconductors and insulators with a semi local exchange-correlation potential. *Phys Rev Lett.* 2009;102(22):226401.
- [32] Blaha P, Schwarz K, Madsen G, Kvasnicka D, Luitz J. *WIEN2K: An augmented plane wave + local orbitals program for calculating crystal propertie.* Vienna, Austria: Vienna University of Technology; 2001.
- [33] Perdew JP, Burke K, Ernzerhof M. Generalized gradient approximation made simple. *Phys Rev Lett.* 1997;77:3865.
- [34] Martin RM. *Electronic structure: basic theory and practical methods.* Cambridge: Cambridge University Press; 2004.
- [35] Kumar A, Verma AS, Bhardwaj SR. Prediction of Formability in Perovskite-Type Oxides. *The Open Applied Physics Journal.* 2008;1:11–19.
- [36] Xu N, Zhao H, Zhou X, Wei W, Lu X, Li F. Dependence of critical radius of the cubic perovskite ABO<sub>3</sub> oxides on the radius of A- and B-site cations. *Int J Hydrog Energy.* 2010;35:7295–7301.
- [37] Sanvito S, Ordejon P, Hill NA. First-principles study of the origin and nature of ferromagnetism in Ga<sub>1-x</sub>Mn<sub>x</sub>As. *Phys Rev B.* 2001;63(16):165206.

## Opto-Electronic Investigation of Rubidium Based Fluoro-Perovskite for Low Birefringent Lens Materials

Iqbal, M. A<sup>1</sup>. and Erum, N.<sup>2,\*</sup>

<sup>1</sup>Department of Physics, University of Management and Technology, Lahore

<sup>2</sup>Department of Physics, University of Punjab, Lahore

\*erum.n@hotmail.com

### Abstract

*In this communication, systematic first principles calculation has been scrutinize to evaluate bonding nature, structural, electronic, and optical properties of RbHgF<sub>3</sub>. The findings are based on total energy calculations where Khon Sham (KS) equation is solved by means of density functional theory (FP-LAPW) method. Optimization of structural parameters is done with variety of approximations, which corroborates through comparison with available experimental data. Assessment of band profile through GGA plus Trans-Blaha modified Becke–Johnson (TB-mBJ) potential highlights underestimation of bandgap with traditional Generalized Gradient approximations. Specific contribution of particular states on electronic properties is investigated by means of total and partial density of states while contour maps of electron density are used to sightsee bonding character and it is evaluated that emphasized compound is (M-I) indirect bandgap material with mixed ionic and covalent bonding character. Additionally attention is paid to absorption and reflection spectra of RbHgF<sub>3</sub>fluoroperovskite by reconnoitering optical properties, which shows extensive absorption and reflection in high frequency regions. Expectantly, current study would benchmark various quantum mechanical effects, which must be taken into account to understand and utilize RbHgF<sub>3</sub> in fabricating practical devices.*

**Keywords:** *first- principles study, fluorine based perovskites, electronic property, optical property*

### Introduction

The knowledge of physical properties of materials is always a principal field of curiosity but in today's hi-tech era trust of potential investors can be strengthened by engrossment of researchers in competition towards higher proficiencies. To fulfill this need material scientists & researchers struggling hard for economical and resourceful materials. The class of compounds having ABF<sub>3</sub> stoichiometry is known as fluoroperovskites. Here A is usually alkali, alkaline or rare earth metals while B is supposed to be transition, post transition and non-transition metals although anion is represented by X that are oxides and halides [1].

In this study emphasize is given to Rubidium based mercury fluoroperovskite which own great technological importance in fabricating low birefringent excellent lens materials, transparent coating devices, opto-electronic & optical pathways, photovoltaic applications, ionic conducting, luminescence capacitor, UV detectors as well as Light Emitting Diodes (LED). Particularly  $\text{RbHgF}_3$  is a superior choice for the high-class lens materials because it does not suffer with birefringence, which can make design of lenses problematic [2-10]. Comprehensive experimental studies are available on their interesting structural properties which is being confirmed that under consideration compound crystallizes in cubic structure and it do not unveil any phase transition under varies pressure and temperature [11-12].

From above literature this idea can be established that focused material is technically sound which motivate us to inquire it in detail. Our main goal is to improve trends of all physical properties concurrently. This paper is schematized in the following sections where Section 1, have already described some introductory details about materials and their applications. Section 2, is devoted to method and computational detail of calculations. Section 3, present results, and discussions of structural and opto-electronic properties. Finally, all results are compared with previous studies where data is available. At the end, we enlighten future prospective of this research.

## 2. Computational Details

The present first principles study have been carried out on the basis of density functional theory (DFT) which is implemented in wien2k code to solve Kohn Sham equation within Full Potential Linearized Augmented Plane Wave (FP-LAPW) method. This method is one of the best methods for appropriate computation of electronic states and optical response of various crystalline solids. For structural optimization the exchange correlation approximation is treated with Perdew-Burke-Ernzerhof Generalized Gradient Approximation (PBE-GGA), Wu Cohen Generalized Gradient Approximation (WC-GGA), PBEsol-GGA and Local Density Approximation (LDA) while for opto-electronic properties recently bugged GGA plus Trans-Blaha modified Becke-Johnson (TB-mBJ) potential is employed [13-16].

In order to enhance accuracy in calculations valence electrons are treated semi-relativistically and core electrons are treated fully relativistically. Convergence in basis size is achieved with a cut-off  $R_{\text{MT}} \cdot K_{\text{max}} = 8.0$ , which is product of smallest muffin-tin radius  $R_{\text{MT}}$  times the largest plane wave vector  $K_{\text{max}}$ . Brillouin zone (BZ) integration is done with 56 K point using modified form of tetrahedron method [17]. The calculations are self-consistently converged when total energy and charge is stable within 0.001mRy and 0.01 m respectively.

Furthermore, to calculate validate optical properties denser mesh of Brillouin zone (BZ) sampling is done with enormous number of K points.

Table1.

Comparison of Present calculation with previous experimental and theoretical values for lattice constants ( $a_0$ ), ground state energies ( $E_0$ ), bulk modulus ( $B_0$ ) and its pressure derivative ( $B_p$ ) of  $RbHgF_3$  compound.

Compound $RbHgF_3$	Present work PBE-GGA	Present work WC-GGA	Present work PBEsol-GGA	Present work LDA	Experi- mental work	Other theoretic al work
$a_0$ (Å)	4.60	4.57	4.53	4.49	4.47 <sup>a</sup>	4.46 <sup>b</sup>
$E_0$ (Ry)	-45854.51	-45854.43	-45854.40	-45854.39		
$B_0$ (GPa)	48.84	49.01	49.39	49.81	48.32 <sup>a</sup>	
$B_p$ (GPa)	5.61	5.58	5.53	5.51		

<sup>a)</sup> Ref.[22] (Experimental work)      <sup>b)</sup> Ref.[23] (Other theoretical work)

### 3. Results and Discussion

#### 3.1. Structural Properties

Ternary fluoroperovskite  $RbHgF_3$  crystallizes itself in cubic type of structure having space group  $Pm3m$  (#221) while its unit cell occupy one molecule. Figure1 illustrates the sites of Wyckoff coordinates which are situated at 1a (0 0 0), 1b (1/2,1/2,0), 3c (0, 1/2, 1/2) for Rb, Hg and F respectively. This subsection is dedicated to calculate structural properties of  $RbHgF_3$  via energy minimization process in which total energy varies as a function of equilibrium cell volume ( $V_0$ ). Accurate total energy versus volume curve is fitted with equation of state (EOS) developed by Murnaghan [18] as shown in Figure2.

Equilibrium lattice constant ( $a_0$ ), ground stata energy ( $E_0$ ), bulk modulus ( $B_0$ ), and pressure derivative of bulk modulus ( $B_p$ ) are calculated with four different exchange and correlation schemes namely PBE-GGA, WC-GGA, LDA and PBEsol-GGA. However from Table1 it can be observed that lattice constant computed by DFT slightly overvalue as compared to experimental data that can be associated due to use of traditional DFT schemes. The value of bulk modulus represents good crystal rigidity in  $RbHgF_3$ fluoroperovskite compound. Furthermore, Table1 depicts contrary relation between lattice constant and bulk modulus in accordance with the trend of other fluoroperovskite compounds [19-21]. As a result all structural parameters are in reasonable agreement with previous theoretical and existing experimental data.

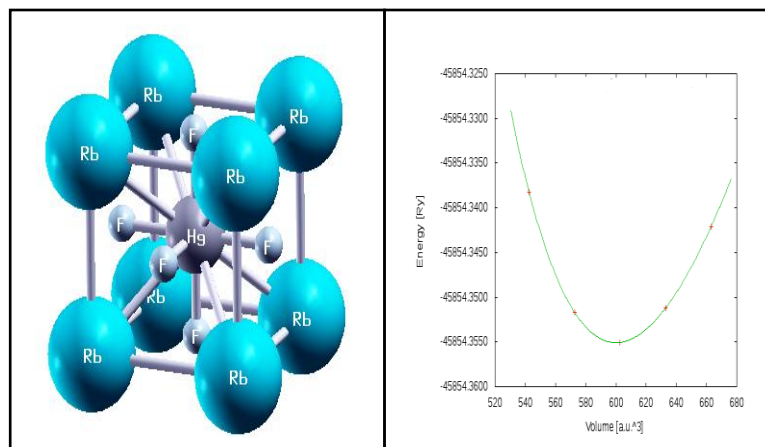


Figure1. Crystal structures of  $\text{RbHgF}_3$

Figure2. Variation of total energy as a function of unit cell volume for  $\text{RbHgF}_3$

### 3.2. Electronic Properties

The electronic properties of  $\text{RbHgF}_3$  fluoroperovskite compound is described in terms of calculating energy band structure and total as well as partial density of states (TDOS and PDOS) whereas bonding nature is evaluated with aid of electron density plots. In this subsection band gap is computed with GGA plus Trans-Blaha modified Becke–Johnson (TB-mBJ) potential in order to avoid underestimation of well-known exchange and correlation scheme of LDA and GGA [24-27]. To clarify this concept bandstructure comparison is made with PBE-GGA scheme to prove this underestimation. The resultant energy bandstructure in high symmetry directions are shown in Figure3 with PBE-GGA and mBJ potential. It can be analyzed from s that overall trend of band dispersion curves are almost same and conduction band minimum (CBM) lies at  $\Gamma$  symmetry point of brillouin zone (BZ) whereas valence band maximum (VBM) is located at M point brillouin zone (BZ) which reveals (M- $\Gamma$ ) indirect bandgap of 3.2 eV and 1.0 eV from mBJ and PBE-GGA schemes respectively. Unfortunately, there is lack of experimental bandgap data to make a reasonable comparison. However, the compound can work well in ultraviolet region of electromagnetic spectrum because the materials with band gaps larger than 3.1 eV work well in the ultraviolet region of the spectrum [28].

Energy density distribution of varied states is observed in terms of total and partial density of states (TDOS & PDOS). According to Figure4-5 it is obvious that TDOS and PDOS of  $\text{RbHgF}_3$  fluoroperovskite compound can be splitted into varied energy regions ranging from -10 eV to 15 eV. A narrow sharp peak is observed at -10 eV due to **Rb-4p** states. The upper region of valence band

from Fermi-level to -6.1 eV is due to overlapping of **Hg-3d** and **F-2p** states. While above Fermi level, lower part of conduction band is occupied by **Hg-4s** and upper part of conduction band is filled by **Rb-4d** states. For the sake of precision in density of states, we omit some distorted peaks which can hinder justification of electronic states.

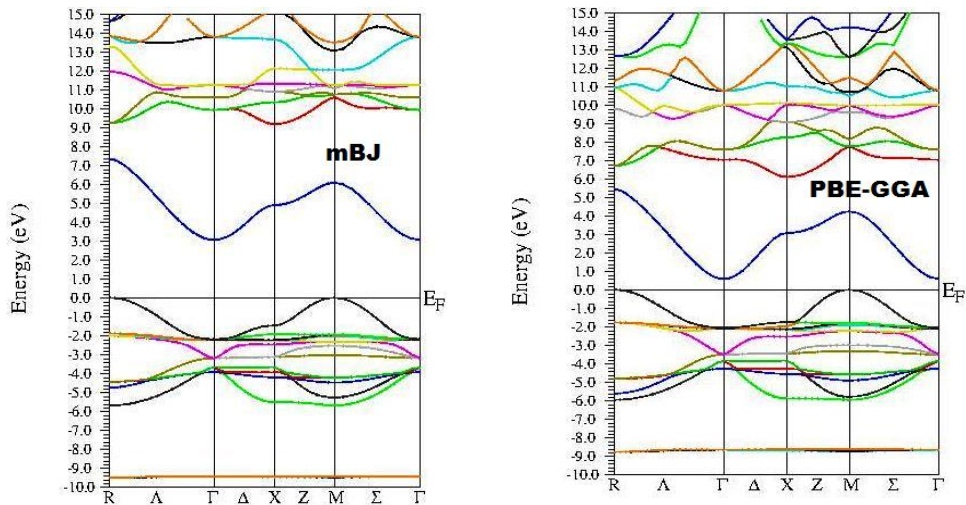


Figure3. Comparison of calculated band structure in high symmetry directions with PBE-GGA & mBj potential

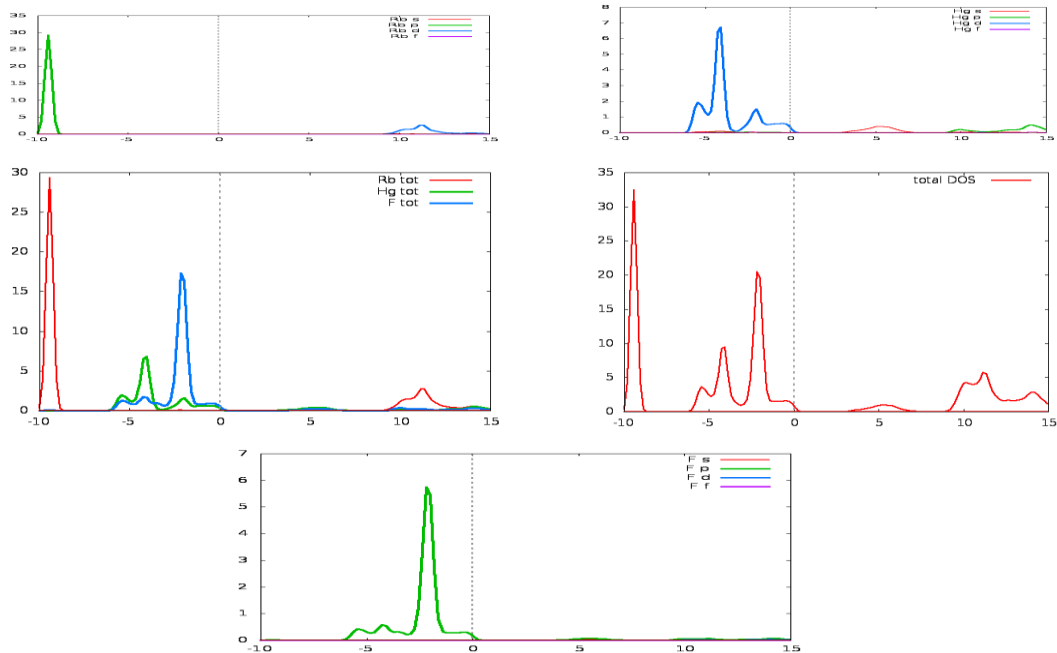
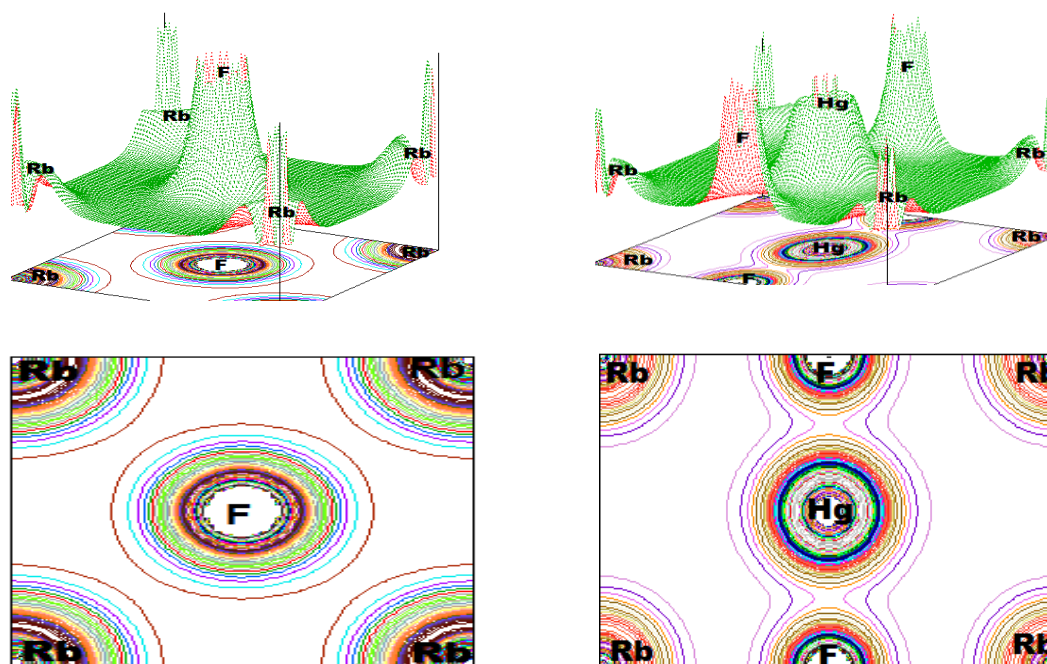


Figure4-5 Calculated total and partial density of states (TDOS & PDOS)



(I) (100) plane

(II) (110) plane

Figure6. Calculated mBJ total two and three dimensional electronic charge densities for (I) in the (100) plane and (II) in the (110) plane.

The maps of contour plots in terms of electron density communicate a crucial role in explaining nature of chemical bond in crystalline materials [29]. The dispersion curves of contour maps are calculated along (100) and (110) planes in 2D along with 3D as quoted in Figure6. The strong ionic nature of Rb-F bond is evident from perfect spherical charge distribution between cation of rubidium and anion of fluorine. The charge is transferred between Rb cation and F anion due to large electronegativity difference in them. On the other hand, uniform distribution is observed between Hg cation and F anion which divulges covalent nature in  $\text{HgF}_3$  octahedra. In fact above analysis synchronizes well with results of DOS Figure4-5 where p-d hybridization is maximum between **Hg-3d** and **F-2p** states. Conclusively our results authorize mixed ionic as well as covalent bonding nature in  $\text{RbHgF}_3$ . Furthermore in Refs. [20,21] similar results of bonding type is observed for other fluoroperovskite compounds.

In order to expose internal behavior of emphasized compound the tool of optical analysis is employed. Fundamental optical responses include imaginary part of dielectric function  $\epsilon_2(\omega)$ , real part dielectric function  $\epsilon_1(\omega)$ . Further analysis is extended to plot optical spectra of absorption coefficient and reflectivity which are crucial in concern with device applications.

The complex dielectric function  $\varepsilon(\omega)$  can break into real and imaginary part according to following relation [30]:

$$\varepsilon(\omega) = \varepsilon_1(\omega) + i\varepsilon_2(\omega) \quad (1)$$

In equation (1)  $\varepsilon_2(\omega)$  denotes imaginary part of dielectric function while  $\varepsilon_1(\omega)$  represent real part of dielectric function. The analysis of  $\varepsilon_2(\omega)$  as shown in Figure7 out complete response of material due to applied electromagnetic radiation. In this study, we highlight results of direct interband transition although summarizing all possible transitions originating from occupied valence band to unoccupied conduction band taking into account appropriate element of transition dipole matrix [31].The widespread peaks of  $\varepsilon_2(\omega)$  follow pattern of DOS and band structure of the investigated compound. The threshold energy point occurs at 5.2 eV approximately while the major peak are located at 5.9 eV which corresponds to transition of occupied valence band states to unoccupied conduction band states. These peaks are majorly due to Hg-4s states. After that diverse peaks are observed till 15eV which occurs due to hybridized states of Rb-4d alongwith some p states of Hg as well as F.

Absorptive behavior of material is analyzed with the help of real part of dielectric function  $\varepsilon_1(\omega)$  as shown in Figure8. At zero frequency limit static part of dielectric function  $\varepsilon_1(0)$  is observed at 1.88 eV. The curves of  $\varepsilon_1(\omega)$  starts increasing and attains a maximum value at around 5 eV and an overall narrow bandgap semiconductive nature is observed.

The plot of absorption coefficient as a function of energy depicts that RbHgF<sub>3</sub> starts absorbing electromagnetic radiation at about 5.25 eV as presented in Figure9. This particular energy is also known as threshold point. This threshold point is exactly in accordance with trend of bandgap. Hereafter oscillations are observed with increasing absorption pattern in spectra. Investigated material starts absorbing effectively within 21-25 eV range while highest prominent peak is observed at around 21.5 eV. After the incnet of optimum absorption peak it again going to decrease suffering trivial variations. Analysis of absorption spectra concludes clearly about application of this fluoroperovskite for absorption purposes in wide range of Ultra-Violet region of electromagnetic spectrum typically at about 21.5 eV.

The calculated spectrum of reflectivity as a function of electromagnetic energy is shown in Figure10. The phenomenon of reflectivity stays below 9-10% upto 20eV. Currently focused material starts reflecting highly and attains maximum value almost at 22eV that helps to understand that by following different regions of electromagnetic spectrum (EM) RbHgF<sub>3</sub> remains highly transparent in infrared (IR) and visible (V) regions which recommends that under

consideration compound is an upbeat candidate for efficient lenses and transparent coating devices.

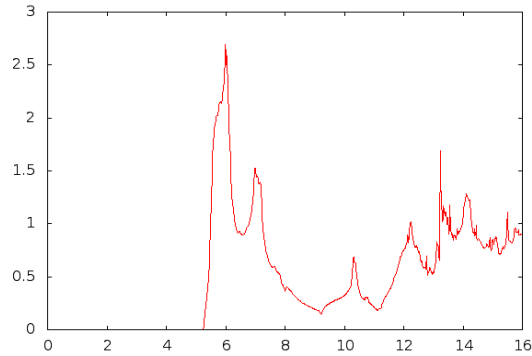


Figure7. Calculated imaginary part  $\epsilon_2(\omega)$  of the di-electric function for RbhgF<sub>3</sub> compound

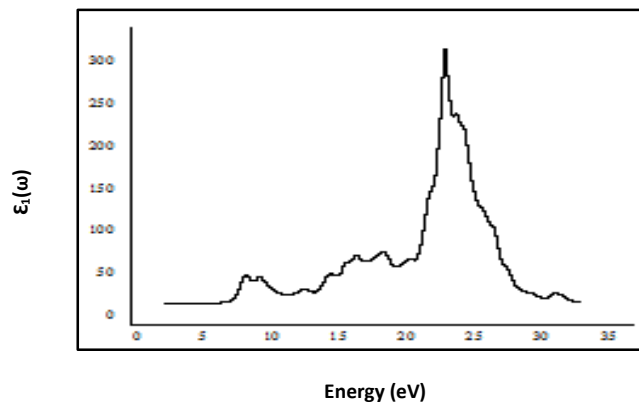
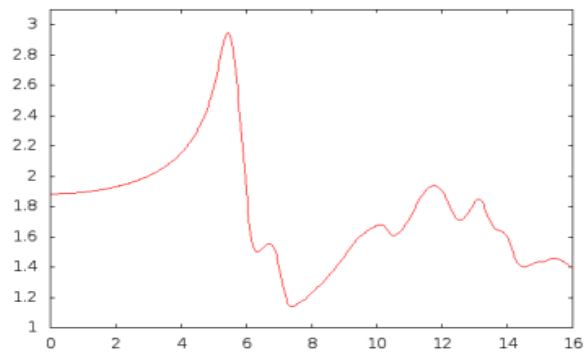


Figure8. Calculated real part  $\epsilon_1(\omega)$  of the dielectric function for RbHgF<sub>3</sub> compound.

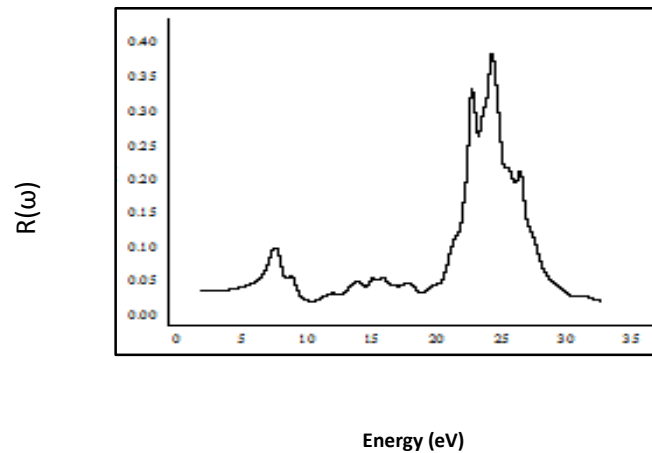


Figure9. Reflectivity  $R(\omega)$  as a function of energy for  $\text{RbHgF}_3$  compound

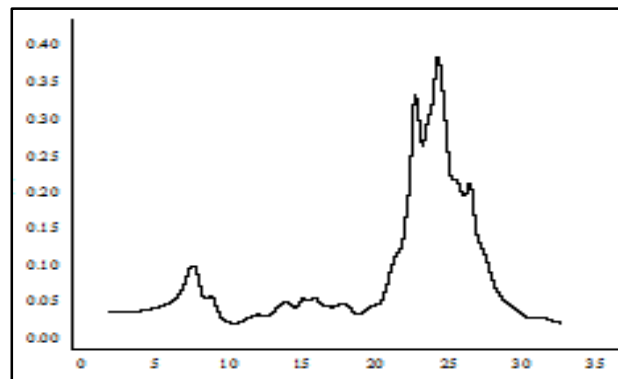


Figure10. Absorption coefficient  $\alpha(\omega)$  as a function of energy for  $\text{RbHgF}_3$  compound

#### 4. Conclusion

In this work, all electron self-consistent Full Potential-Linearized Augmented Plane Wave (FP-LAPW) method is used to explore structural, electronic, and optical properties of  $\text{RbHgF}_3$  fluoro-perovskite compound. In order to inspect optimized structural parameters exchange-correlation contribution is treated with four different approximations. To elude underestimation of band profile by other DFT schemes we highlight GGA plus Trans-Blaha modified Becke–Johnson (TB-mBJ) potential in lieu of attaining opto-electronic results near to expected experimental findings. Energy band profile confirms that investigated material is a narrow and indirect energy bandgap ( $M-\Gamma$ ) semiconductor. The total and partial density of state curves is used to define

contribution of different bands. In addition to its contour maps of electron density authenticates mixed covalent-ionic behavior. These results are in favorable agreement with previous theoretical and existing experimental data. The optical properties are discussed in terms of advantageous functional parameters and analysis is being done by interband contribution that shows  $\text{RbHgF}_3$  possess wide range of absorption and reflection in high frequency regions and these characteristics make them useful for transparent coatings and fabricating low birefringent high-quality lenses. Conclusively limelight fluoroperovskite can efficiently be used for fabricating high-class low birefringent lens material and photovoltaic applications.

### References

- [1] Lang L, Yang J, Liu H, Xiang HJ, Gong XG. First-principles study on the electronic and optical properties of cubic  $\text{ABX}_3$  halide perovskites. *Phys Lett A*. 2014;378(3):290–293.
- [2] Vaitheeswaran G, Kanchana V, Svane A, Delin A. High-pressure structural study of fluoroperovskite  $\text{CsCdF}_3$  up to 60 GPa: A combined experimental and theoretical study. *J Phys: Condens Matter*. 2007;19:326214.
- [3] Eibschutz M, Guggenheim HJ, Wemple SH, Camlibel I, Didomenico M. Ferroelectricity in  $\text{BaM}_{2+2}\text{F}_4$ . *Phys Lett*. 1969;7:409.
- [4] Horsch G, Paus HJ. A new color center laser on the basis of lead doped  $\text{KMgF}_3$ . *Opt Commun*. 1986;60:69.
- [5] Salehi H. First Principles studies on the electronic structure and band structure of paraelectric  $\text{SrTiO}_3$  by different approximations. *J Mod Phys*. 2011;2:934–943.
- [6] Slassi A. Ab initio study of a cubic perovskite: Structural, electronic, optical and electrical properties of native, lanthanum and antimony-doped barium tin oxide. *Mater Sci Semicond Process*. 2015;32:100–106.
- [7] Chadwick AV, Strange JH. *Studies of ionic motion in perovskite fluorides*. In: Gesellschaft DP, editor. *Physikalische Berichte*, vol 6. Berlin: Physik Verlag; 1983. p. 9–10, 555–558.
- [8] Vaills Y, Buzare JY. X-ray investigations of the cubic to tetragonal phase transition in  $\text{CsCaCl}_3$  at  $T_c = 95$  K. *Solid State Commun*. 1986;60:139–141.
- [9] Mitchell RH. *Perovskites: Modern and ancient*. Thunder Bay, Ont., Canada: Almaz Press; 2002.

- [10] Huang K, Feng M, Goodenough J, Milliken C. Double perovskites as anode materials for solid oxide fuel cells. *J Electrochem Soc.* 1997;144:3620.
- [11] Ihringer J, Maichle J, Prandl W, Hewat A, Wroblewski T. Crystal structure of the ceramic superconductor  $\text{BaPb}_{0.75}\text{Bi}_{0.25}\text{O}_3$ . *Zeitschrift Fur Physik B-Condensed Matter.* 1991;82:171.
- [12] Dotzler C, Williams GV, Edgar A. Radiation-induced optically and thermally stimulated luminescence in  $\text{RbCdF}_3$  and  $\text{RbMgF}_3$ . *Curr Appl Phys.* 2008;8:447.
- [13] Schwarz K, Blaha P. Solid state calculations using Wien2k. *Comput Mat Sci.* 2003;28:259–273.
- [14] Blaha P, Schwarz K, Madsen GK. Electronic structure calculations of solids using the WIEN2k package for material sciences. *Comput Phys Commun.* 2002;147:71–76.
- [15] Kohn W, Sham LJ. Self-consistent equations including exchange and correlation effects. *Phys Rev.* 1965;140:1133.
- [16] Tran F, Blaha P. Accurate band gaps of semiconductors and insulators with a semilocal exchange-correlation potential. *Phys Rev Lett.* 2009;102:226401.
- [17] Khetre SM, Jadhav HV, Jagadale PN, Kulali SR, Bamane SR. Studies on electrical and dielectric properties of  $\text{LaFeO}_3$ . *Adv Appl Sci Res.* 2011;2:503–511.
- [18] Murnaghan FD. The compressibility of media under extreme. *Pressures Proc Natl Acad Sci USA.* 1994;3:244.
- [19] Ghebouli B, Ghebouli MA, Bouhemadou A, Fatmi M, Khenata R, Rached D, et al. First principles study of the structural, elastic, electronic, optical and thermodynamic properties of the cubic perovskite  $\text{CsCdCl}_3$  under high pressure. *Solid State Sci.* 2012;14:903.
- [20] Rose SK, Satpathy S, Jepsen O. Semiconducting  $\text{CsSnBr}_3$ . *Phys Rev B.* 1993;47:4276–4280.
- [21] Brik MG. Comparative first-principles calculations of electronic, optical and elastic anisotropy properties of  $\text{CsXBr}_3$  ( $\text{X}=\text{Ca}, \text{Ge}, \text{Sn}$ ) crystals. *Solid State Commun.* 2011;151:733–1738.
- [22] Muller O, Roy R. *The major ternary structural families.* New York: Springer; 1974.

- [23] Moreira RL, Dias A. Comment on prediction of lattice constant in cubic perovskites. *J Phys Chem Solids*. 2007;68:1617.
- [24] Berastegui P, Hull S, Eriksson SG. A low-temperature structural phase transition in CsPbF<sub>3</sub>. *J Phys: Condens Matter*. 2001;13(22):5077.
- [25] Reshak AH, Chen X, Auluck S, Kamarudin H. DFT calculation for elastic constants of orthorhombic structure within WIEN2K code: A new package (ortho-elastic). *J Appl Phys*. 2012;112:053526.
- [26] El Haj Hassan F, Akbarzadeh H. First-principles elastic and bonding properties of barium chalcogenides. *Comput Mater Sci*. 2006;38:362–368.
- [27] Reshak AH, Kamarudin H, Auluck S. DFT calculation for elastic constants of orthorhombic structure within WIEN2K code: A new package (ortho-elastic). *J Phys Chem B*. 2012;116:4677.
- [28] Luana V, Costales A, Pendas AM, Florez M, Fernandez VM. Structural and chemical stability of halide perovskites. *Solid State Commun*. 1997;104:47–50.
- [29] Kittel C, *Introduction to solid state physics*. 8th ed. New York: John Wiley & Sons; 2005.
- [30] Fox, optical properties of solids. New York: Oxford University Press; 2001.
- [31] Kumar S, Maury TK, Auluck S. Correlation between ionic charge and the lattice constant of cubic perovskite solids. *J Phys: Condens Matter*. 2008;20:075205.

## Analysis of Non-polar Chemical Profile of *Melia Azedarach* L.

Habib, R.<sup>1</sup>, Mohyuddin, A<sup>1</sup>., Khan, Z<sup>2</sup>. and Mahmood, T<sup>3</sup>.

<sup>1</sup>Department of Chemistry, University of Management and Technology, Lahore

<sup>2</sup> Department of Botany, GC University, Lahore

<sup>3</sup>Central Research Lab, Lahore College for Women University, Lahore

\*rabiraho@gmail.com,

### Abstract

*Medicinal plants are conventionally used for the treatment of various diseases due to their world-wide occurrence and least side effects. Melia azedarach L. belongs to the family Meliaceae, is a highly significant medicinal plant. Extracts of M. azedarach obtained from its different parts such as seed, fruit, flower, leaf, and young branches are reported to exhibit antifungal, antihelmintic, nematicidal, diuretic, cytotoxic, antiproliferative, insecticidal and antioxidant activities. Thus the aim of this study was to explore the chemical profile of non-polar extract of M. azedarach leaves through GC-MS analysis. The identification of phytochemical compounds is based on molecular ion peak, base peak, and fragmentation pattern. GC-MS analysis of hexane extract of M. azedarach showed a highly complex profile, containing ketones, ethers, fatty acid derivatives, methyl esters, 1,3-dipalmitate, 7,8-dihydrocarpesterol, and 2-Undecanol. This study will be useful to explore the active components of medicinal plants and can validate their medicinal value.*

**Keywords:** *Melia azedarach* L., Meliaceae, GC-MS method, Phytochemical compound.

### Introduction

There is an increasing demand for the herbal medicine to cure variety of diseases as these medicines are efficient and safe without any side effects as compared to synthetic drugs [1]. For this purpose, scientist, botanists, chemists, and pharmacists all over the world are working on herbal medicines [2]. *Melia azedarach* Linn. (*M. azedarach*) commonly known as chinaberry or Persian lilac tree is a plant species of the family *Meliaceae* that contain 45 genus and 750 species. It is deciduous tree of medium sized that grows to a height of five to fifteen meter tall and thirty to sixty cm in diameter. It can be grown successfully in a wide variety of situations even in alkaline soil where other trees might fail to grow. It is native to Indochina, Pakistan, India, Australia, and Southeast Asia. It is cultivated in most of the countries located in tropics and subtropical region. This plant has long been known as an insecticidal and medicinal plant all over the world due to its world-wide availability and fewer side effects. Extracts of *M.*

*azedarach* obtained from its different parts such as seed, fruit, flower, leaf, and young branches have been used for the treatment of diabetes, malaria, intestinal worms, cough, nausea, vomiting and paroxysmal fever, and skin disease [3-5].

GC-MS has been known as a powerful technique for providing metabolic profiling of plants [6-9]. Hexane extracts of many species of *Meliaceae* family are analyzed by this technique but there has been no report on GC-MS of hexane extract of *M. azedarach* or any species of genus *Melia*. *Non polar profile of M. azedarach* has not been explored yet. Therefore, the aim of the study was to explore the chemical profile of non-polar extract of *M. azedarach* leaves through GC-MS analysis.

## 2. Material and Methods

**2.1. Preparation of plant extract:** The fresh leaves of plant *M. azedarach* was collected from the Botanical Garden of Government College University, Lahore and washed individually to remove impurities and dried under shade. Dried leaves were crushed into fine powder using a grinder.

The dried plant powder were weighed and dipped in a hexane and left for seven days. The hexane extract was then filtered. The hexane extract was concentrated under reduced pressure and low temperature in a Rotary Evaporator. The semi solid extract were obtained.

**2.2. Phytochemical analysis of plant extract:** Phytochemical analysis were carried out by employing standard procedures to sort out the presence of flavonoids, alkaloids, tannins, saponins and steroids in hexane extract of *Melia azedarach* [10, 11].

**2.3. Preparation of sample for GC/MS analysis:** A measured amount of semi solid was re-dissolved in *n*-hexane of GC grade and micro-filtered to prepare the samples of 5.0 mg /10 mL.

**2.4. Gas Chromatography Mass Spectrometry analysis:** A GC-MS analysis was carried out on a Shimadzu GCMS-QP2010A system in EI mode (70 eV) with DB-5MS capillary column (30 m × 0.25 mm i.d., film thickness: 0.25 µm, J and W scientific, Fulsom, CA, USA. 1 µL of samples were injected at 250 °C with a split ratio of 50/50 under electronic pressure to maintain a constant flow (0.67 mL/min) of the helium carrier gas. The oven temperature was programmed from 150 °C for 4 min and heated to 300 °C at a rate of 3 °C/min and kept constant at this temperature for 2 min. The mass spectrometer was set to scan the mass range 40-600 amu with ion source temperature 200 °C and interface temperature was 250 °C. Analyses were performed in triplicate with a blank run after every analysis. The resulting data was interpreted by using Shimadzu Lab Solution, GC-MS Postrun analysis software. Compounds were identified by comparing the ions

fragmentation pattern of mass spectra with those of known compounds stored in NIST 147 and NIST 127 libraries.

### 3. Results and Discussion

The genus *Melia* is famous for the presence of liminoids and terpenoids that are water-insoluble plant components [12]. Previous researches have proved that these compounds have diverse effect against pathogens. Moreover, non polar profile of *M. azedarach* has not been explored yet. The waxy coating of leaves can only be dissolved by non polar solvent because waxes are non polar in nature. Therefore, the leaves of *M. azedarach* were extracted with n-hexane in order to isolate the wax.

**3.1. Phytochemical analysis of plant extract:** The phytochemical analysis was carried out and it was seen that alkaloids and flavonoids are absent in hexane extract of *M. azedarach*, whereas it contain tannins, terpenes, quinines, saponins and steroids as given in Table1.

Table1.  
Phytochemical Analysis

Experiment	Observation	Inference
<b>Test for Alkaloids</b>		
Mayer's test	No yellow ppt.	Alkaloids absent
Wagner's test	No reddish brown ppt. No cloudy appearance	Alkaloids absent
Dragendorff test	Bluish green ppt.	Alkaloids absent
<b>Test for Tannins</b>		
5ml extract + 6 drops FeCl <sub>3</sub>	Yellow florescence	Tannins present
<b>Test for Coumarins</b>		
plant extract+ 1N NaOH+ Pass through Uvlight	yellow florescence is not produced	Coumarins present
<b>Test for Flavonoids</b>		
Plant extract +2ml AlCl <sub>3</sub>	Persistent froth	Flavonoids absent
<b>Test for Saponins</b>		
Shook the aqueous plant vigorously	Violet color	Saponins present
<b>Test for Steroids</b>		
Leibermann-Burchard test	Red color	Steroids present
<b>Test for Anthraquinon</b>		
Plant extract + few drops N,N- dimethylaniline		Anthraquinones present

**3.2. Gas Chromatography Mass Spectrometry analysis:** Gas Chromatography and Mass spectroscopy analysis of compounds was carried out in n-hexane leaf extract of *M. azedarach* (Figure1).

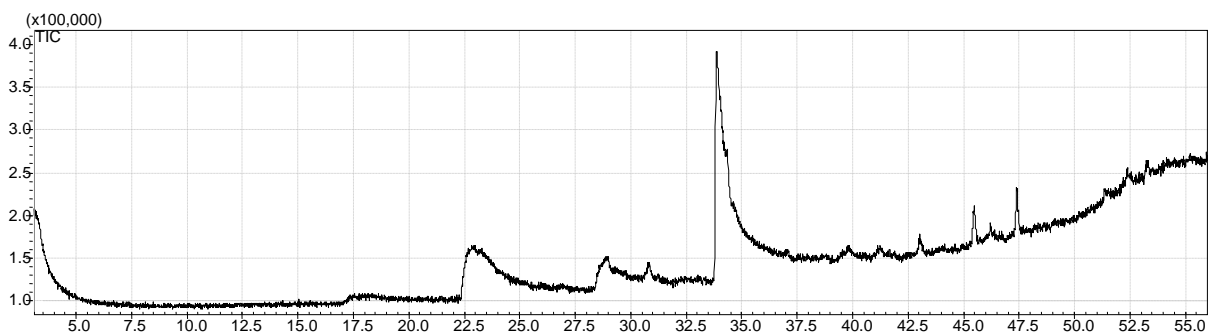


Figure1. GC chromatogram of *n*-hexane extract of *M. azedarach* leaves

Different compounds were identified in the hexane extract of *M. azedarach* on the basis of retention time, molecular ion peak, base peak, and mass fragmentation pattern. Eight peaks from non-polar plant extract were identified as: 2-Undecanol, Methyl 4, 6-decadienyl ether, 13-Docosenoic acid, 7, 8-Dihydrocarpesterol, Glutaric acid, dimethyl ester, Nonanoic acid, 1, 2, 3-propanetriyl ester, Glycerol 2-acetate 1, 3-dipalmitate and Docosenoic acid, 1 methyl-butyl ester as shown in Table2.

Table2.

Compounds from hexane extract of *M. azedarach*

Name of compound	Retention Time (mins)	Base Peak (m/z)
2-Undecanol	22.39	45
Methyl 4, 6-decadienyl ether	22.45	45
13-Docosenoic acid	33.88	55
7, 8-Dihydrocarpesterol	45.48	414
Glutaric acid, dimethyl ester	47.24	133
Nonanoic acid, 1, 2, 3-propanetriyl ester	52.09	151
Glycerol 2-acetate 1, 3-dipalmitate	52.18	40
Docosenoic acid, 1 methyl-butyl ester	54.90	44

2-Undecanol was eluted at 22.39 min. Base peak of the compound was observed at m/z 45. The fragment ions observed m/z 40, 60, 83, 97, 150. The fragment ion observed at m/z 83 was due to the loss of -CH<sub>2</sub> group from molecular ion (M<sup>+</sup>). Methyl 4, 6-decadienyl ether was eluted at 22.45 min. Base peak of the compound was observed at m/z 45. The fragment ions observed m/z 41, 56, 70, 84, 150. The fragment ion observed at m/z 70 was due to the loss of -CH<sub>2</sub> group from M<sup>+</sup>. 13-Docosenoic acid was eluted at 33.88 min. Base peak of the compound was observed at m/z 55. The fragment ions observed m/z 69, 83, 97, 185, 207, 320. The fragment ion observed at m/z 83 was due to the loss of -CH<sub>2</sub> group from M<sup>+</sup>. 7, 8-Dihydrocarpesterol was eluted at 45.48 min. Base peak of the compound was observed at m/z 441. The fragment ions observed at m/z 91,

133, 147, 191, 208, 335, 441. The fragment ion observed at m/z 191 was due to the loss of -OH group from M<sup>+</sup>. Glutaric acid, dimethyl ester was eluted at 47.24 min. Base peak of the compound was observed at m/z 133. The fragment ions observed m/z 40, 69, 83, 193, 209, 281. The fragment ion observed at m/z 40 was due to the loss of -C<sub>2</sub>H<sub>5</sub> group from M<sup>+</sup>. Nonanoic acid, 1, 2, 3-propanetriyl ester was eluted at 52.09 min. Base peak of the compound was observed at m/z 151. The fragment ions observed m/z 44, 68, 85, 100, 169, 207, 281, 335. The fragment ion observed at m/z 68 was due to the loss of -OH group from M<sup>+</sup>. Glycerol 2-acetate 1, 3-dipalmitate was eluted at 52.18 min. Base peak of the compound was observed at m/z 40. The fragment ions observed m/z 68, 100, 169, 209, 267, 335, 441. Docosenoic acid, 1 methyl-butyl ester was eluted at 54.90 min. Base peak of the compound was observed at m/z 44. The fragment ions observed m/z 77, 101, 137, 150, 208, 341. The fragment ion observed at m/z 177 was due to the loss of -CH<sub>3</sub> group from M<sup>+</sup>.

### Conclusion

Traditionally, medicinal plants are largely used to cure many diseases owing to their least side effects. *M. azedarach* L. belongs to potent medicinal plant family *Meliaceae*. This was the first report on GC-MS of Hexane extract of *M. azedarach*. The results showed that non polar extract of the plant contained a variety of compounds such as ketones, ethers, fatty acid derivatives, methyl esters, 1,3-dipalmitate, 7,8-dihydrocarpesterol, and 2-Undecanol. This will contribute in completing the chemical profile of *M. azedarach*.

### References

- [1] Hariprasad PS, Ramakrishnan N. GC-MS analysis of *Rumex vesicarius* L. *Int J Drug Dev Res.* 2011;3(2):256–263.
- [2] Walli TE. *Text book of pharmacognosy.* 2<sup>nd</sup> Ed. London: J and A Churchill; 1951.
- [3] Azam MM, Mamun-Or-Rashid AN, Towfique NM, Sen MK, Nasrin S. Pharmacological potentials of *Melia azedarach* L. A review. *Am J BioSci.*2013;1(2):44–49.
- [4] Sultana S, Akhtar N, Asif HA. Phytochemical screening and antipyretic effects of hydro-methanol extract of *Melia azedarach* leaves in rabbits. *Bangladesh J Pharmacol.* 2013;8(2):214–217.
- [5] Nadkarni KM. *Indian Materia Medica.* Bombay: Popular Prakashan;1954. 784–785 p.
- [6] Fernie AR, Trethewey RN, Krotzky AJ, Willmitzer L. Metabolite profiling: from diagnostics to systems biology. *Nat Rev Mol Cell Biol.* 2004;5(9):763–769.
- [7] Sumner LW, Mendes P, Dixon RA. Plant metabolomics: largescale phytochemistry in the functional genomics era. *Phytochemistry.* 2003;62(6):817–836.
- [8] Fiehn O. Metabolomics – the link between genotypes and phenotypes. *Plant Mol Biol.* 2002;48(1–2):155–171.
- [9] Kell DB, Brown M, Davey HM, Dunn WB, Spasic I, Oliver SG. Metabolic footprinting and systems biology. *Nat Rev Microbiol.* 2005;3(7):557–565.
- [10] Emeruwa AC. Antimicrobial substances from *Carica papaya* fruit extracts. *Journal of Natural Products.* 1982;45(2):123–127.
- [11] Evans WC. *Trease and Evans Pharmacognosy.* 5<sup>th</sup> Ed. Edinburgh: Saunders Elsevier; 2002.
- [12] Satyavati GV, Raina MK, Sharma M, Editors. *Medicinal Plants of India.* New Delhi: Indian council of medical research; 1976. 201–206 p.

## Table of Contents

1	<b>2nd -Order Parallel Splitting Methods for Heat Equation</b> <i>Aziz, M. and Rehman, M. A.</i>	1
2	<b>Generalization of Topsis from Soft Set to Fuzzy Soft Sets in Decision Making Problem</b> <i>Saeed, M., Anam, Z., Kanwal, T. Saba, I. Memoona, F. and Tabassum, M. F.</i>	11
3	<b>Exploration of antibacterial potential of <i>Melia azedarach</i> L.</b> <i>Munir, T.I, Mohyuddin, A., Khan, Z. and Haq, R.</i>	19
4	<b>DFT-Mbj Study of Electronic and Magnetic Properties of Cubic CeCrO<sub>3</sub> Compound: An Ab-Initio Investigation</b> <i>Rashid, M., Iqbal, M.A., and Noor, N. A.</i>	27
5	<b>Opto-Electronic Investigation of Rubidium Based Fluoro-Perovskite for Low Birefringent Lens Materials</b> <i>Iqbal, M. A. and Erum, N.</i>	37
6	<b>Analysis of non-polar chemical profile of <i>Melia azedarach</i> L.</b> <i>Habib, R., Mohyuddin, A. Khan and Mahmood, Z. T.</i>	49

**SIR**  
Scientific Inquiry and Review

School of Science  
University of Management and Technology  
C-II Johar Town, Lahore-54770, Pakistan  
UAN: +92 42 111 300 200, Fax: +92 42 35212819  
Email: info.sir@umt.edu.pk



ISSN 2521-2427 (Print)



ISSN 2521-2435 (Online)